EUROPEAN SCHOOL OF MOLECULAR

MEDICINE

NAPLES SITE – *Scientific Coordinator*

Prof. Francesco Salvatore

UNIVERSITA' DEGLI STUDI DI NAPOLI

"FEDERICOII"

Ph.D. in Molecular Medicine
curriculum Molecular Oncology
XX Ciclo

miR34a targets the Notch pathway in medulloblastoma

Supervisor: **Ph.D. student:**

Prof. Massimo Zollo   Emilio Cusanelli

Internal Supervisor:

Prof. Alfredo Fusco

External Supervisor:

Prof. Olivier Delattre

Table of contents

List of abbreviations

MB: Medulloblastoma

LCA: large-cell/anaplastic

VZ: ventricular zone

RL: Rombic lip

GNP: Granular neuronal progenitor cells

NSC: neuronal stem cells

EGL: External granular layer

IGL: internal granular layer

CNS: central nervous system

Shh: Sonic Hedgehog

NBCCS: nevoid basal-cell carcinoma

DLL1: Delta-like protein 1

Jag1: Jagged 1

NICD: Notch intracellular domain

Hes1: Hairy and enhancer of split 1

CSL: CBF1, Su(H) and LAG1 transcription factor

miRNA: microRNA

mRNA: messenger RNA

RISC: RNA-induced silencing complex

Ago: Argonaute protein

UTR: untraslated region

m7G cap: 7-methyl cap

IRES: internal ribosome entry site

EST: expressed sequence tag

ORF: open reading frame

Doxo: doxorubicin

RT-PCR: real-time PCR

miR34a-2'-O-Me: miR34a-2-O-Methyl antisense oligoribonucleotide

un-2'-O-Me: unrelated-2-O-Methyl antisense oligoribonucleotide

Figures index

Table index.

Abstract

Medulloblastoma (MB) is a highly aggressive cancer that mostly affects children, through developmental impairment of the cerebellum. Several miR34a targets belong to the Notch pathway, a signaling pathway that is involved in cerebellum development and that is aberrantly activated during MB tumorigenesis. We show here that miR34a over-expression transiently down-regulates the Notch ligand Delta-like 1 (DLL1) protein levels and also results in Notch1 activation and Notch2 signaling inhibition, an effect that we see in the MB Daoy and D283-MED cells. Moreover, ectopic expression of miR34a in MB cells results in impairment of proliferation rate and soft agar colony formation, while inducing apoptosis and differentiation processes. Noteworthy, the induction of apoptosis was inhibited by ectopic expression of DLL1, suggesting the involvement of DLL1 down-regulation in this process. We also provide evidences that the endogenous expression of miR34a can down-regulate DLL1 protein levels and contribute to the p53-induced apoptosis in Daoy cells, upon doxorubicin stimulation. Induction of miR34a correlates with DLL1 protein down-regulation also in neuroblastoma and breast cancer cells and expression of miR34b and miR34c can contribute to the DLL1 down-regulation. Finally, we report that miR34a, miR34b and miR34c, are down-regulated in human MB tumors. These results suggest that miR34a has an onco-suppressor function in MB and that it can thus be targeted for future therapeutic applications.

INTRODUCTION

Medulloblastoma

Medulloblastoma (MB) a highly invasive embryonal tumor of the cerebellum. It is the most common malignant brain tumor in children and accounts for more than 25% of childhood cancer-related deaths (Wang et al., 2008)

MB occurs bimodally, with peaks of incidences between 3 and 4 years and 8 and 9 years of age, even if can also arise in adults, showing the highest incidence at 20-34 years of age (Crawford et al., 2007). Patients with MB generally show symptoms of obstruction of cerebrospinal fluid flow and cerebellar disfunction including macrocephaly, vomiting and ataxia (Crawford et al., 2007).

MB is currently classified in several variants: classic, desmoplastic, anaplastic, large-cell MB and the MB with extensive nodularity (Gilbertson & Ellison, 2008).

Classic tumors are composed of small round or ellipsoid cells with a high nuclear-to-cytoplasmic ratio, showing scant cytoplasm and dense hyperchromatic nuclei.

The desmoplastic variant is composed of highly proliferative, densely packed and reticulin reach areas that surround reticulin-free nodules. This variant represents 50% of adult cases of MB and 15% of children related cancer.

Desmoplastic medulloblastomas encompass the nodular/desmoplastic MB and the medulloblastoma with extensive nodularity, which contribute approximately 7% and 3% of all medulloblastomas, respectively.

Since all large-cell medulloblastomas have regions of anaplasia, anaplastic and large-cell tumors, accounting for almost 10%-22% and 2%-4% of all medulloblastomas, respectively, are often grouped as large-cell/anaplastic (LCA) medulloblatomas, which represents the most malignant variant (Gilbertson & Ellison, 2008).

Most medulloblastomas are confined to the posterior fossa, however all of the variants can metastasize and 11-43% of patients show disseminated disease either along the craniospinal axis, or, more rarely, to extraneural sites (Crawford et al., 2007).

Disease dissemination rate, patient age and post-operative residual mass represent the most important prognostic markers for MB tumors.

MB patients are indeed divided into risk-stratification groups with patients older than 3 years and gross or near-total surgical tumor resection assigned to the average-risk category, which accounts for 60%-70% of all MB patients; and patients with disseminated disease at presentation or greater than 1.5 cm^2 of residual tumor mass identified as high-risk category. A third stratification scheme is used for patients younger than 3 years old, who generally have worse outcomes mostly due to the increased risk of metastatic disease at presentation, increased rate of subtotal resection, and not receiving craniospinal radiation therapy (Crawford et al., 2007).

Risk-adapted treatments are currently adopted in the management of the MB, including surgical tumor resection, radiotherapy and chemotherapy.

Surgery represents the first approach and a fundamental part of MB treatment. It's aimed to the maximal tumor resection and has shown clear effects of survival improvement, particularly in patients with localized disease (Rutkowski et al., 2005).

Addition of radiation therapy to the surgery, has allowed an overall improvement of MB patients survival. However, craniospinal axis irradiation often results in severe deleterious effects, particularly in infants, thus it is delayed or not given to children younger than 3 years (Crawford et al., 2007).

MB patients belonging to all risk-groups are also commonly treated with chemotherapeutic drugs, including vincristine, cyclophosphamide, etoposide and methotrexate. For younger patients, chemotherapy is widely used as the initial treatment, aimed to delay or avoid radiation therapy. Indeed, intensive postoperative chemotherapy alone showed promising results for treatment of young children without initial metastases (Rutkowski et al., 2005).

Other therapeutic approaches include the use of myeloablative doses of chemotherapy followed by autologous stem cell rescue. Early studies have reported a survival improvement for patients with high-risk medulloblastoma; however, 15% of patients died of treatment-related toxicity (Perez-Martinez et al., 2005).

Relapse of MB generally manifest within 2 years from the initial therapy in infant, and upon 5 years in adults. The management of patients with relapsing disease varies and depends on a range of factors including the age of the patient and the dissemination rate of the disease. However, surgery and possible combined use of chemotherapy and radiotherapy represent the leading therapeutic approach (Crawford et al., 2007).

The employment of multimodality treatment regimens has significantly improved survival rates for MB. However, although patients belonging to the average-risk category show an overall survival rate approaching 70% to 80%, the high-risk patients are generally associated to a very poor prognosis, and MB results still incurable for more then one third of patients. Moreover, survivors commonly suffer of severe long-term side effects due to the aggressive treatments (Crawford et al., 2007; Gilbertson & Ellison, 2008).

Neurocognitive defects are one of the most pervasive of all long-term effects and occur across all age groups. Despite receiving reduced doses of intracranial radiation, younger patients generally have a worse outcome and can show significant declines in intelligence quotient (IQ), correlated with the total dose of radiotherapy and the patient age (Perez-Martinez et al., 2005). The possibility to develop endocrinopathies and secondary malignancies, including high-grade brainstem gliomas, cerebral gliomas, and meningiomas is also a long-term concern for patients treated with radiation therapy (Crawford et al., 2007).

Surgery may also be associated with temporary or permanent neurologic worsening due to postoperative infection and direct brain or cerebellar damage. Moreover, nearly 25% of patients show symptoms of the postoperative cerebellar mutism syndrome. This syndrome of delayed onset, typically hours after surgery, presents with mutism, and can persist for

days or months. The etiology of posterior fossa mutism is still unclear (Crawford et al., 2007).

The tumor's cell of origin and the cellular pathways active in MB tumorigenesis are believed to play a crucial role in the prognosis and possibly response to therapy of MB (de Bont et al., 2008).

Therefore, a better understanding of the pathology and molecular biology of medulloblastoma tumorigenesis is necessary, to identify more efficient therapeutic approaches, thereby improving survival and quality of life of MB patients.

Pathogenesis of MB

The origins of MB are intimately related to the cerebellum development. Indeed, although the precise tumor initiating cells are still to be defined, MB can originate from progenitor cells and neuronal stem cells of the cerebellum (Yang et al., 2008), and pathways regulating the normal cerebellum development play a crucial role in the MB tumorigenesis (Marino, 2005).

Three distinct germinal zones are involved in cerebellum development: the ventricular zone (VZ), the rombic lip (RL) and the white matter (Lee et al., 2005; Wang & Zoghbi, 2001).

Most of the cerebellum cell types, including Purkinjie cells and neurons, such as stellate, basket and Golgi interneurons, generate from multipotent neuronal stem cells (NSCs) of the ventricular zone (VZ); on the other hand cerebellar granule neurons, the most abundant neurons of the brain, develop from a second germinal zone, known as the rhombic lip (Wang & Zoghbi, 2001).

During embryonic development, granule neuron precursor cells (GNPs) of the rombic lip proliferate and migrate over the surface of the cerebellum, generating the external granular layer (EGL). GNPs then migrate inward and differentiate into granule neurons, which form the internal granular layer (IGL) (see Fig.1). The EGL persists until postnatal day (P) 15 in the mouse and into the second postnatal year in the human (Lee et al., 2005). A third stem cell population has been isolated from the white matter of the postnatal cerebellum. These cells can give rise to astrocytes, oligodendrocytes and neurons, but not granule cell neurons (Lee et al., 2005).
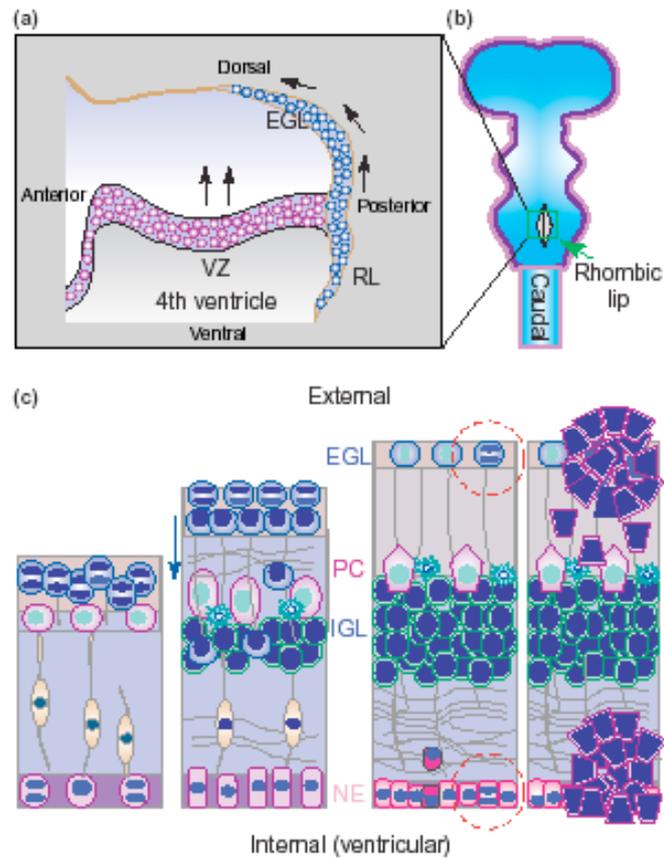
Figure 1. Schematic representation of cerebellar development. (a), (b) *Embryonal development. Progenitor cells located in the ventricular zone (VZ, primary genrminal zone) migrate radially to give rise to Purkinje cells. Progenitor cells located in the rhombic lip (RL) migrate dorsally to populate the external granular layer (EGL, secondary germinal zone). (c) Postnatal development. Progenitor cells located in the EGL clonally expand, become postmitotic, differentiate and migrate inwards to generate the internal granular layer (IGL). Golgi, basket and stellate neurons are originating from the neuroepithelium (NE) of the ventricular zone. The site of origin of medulloblastoma (EGL and NE) is shown on the right-hand side.* **From (Marino, 2005)**

Emerging evidences indicate that MB tumors can generate from either GNPs or NSCs, upon activation of the Sonic Hedgehog (Shh) signaling (Yang et al., 2008).

Shh, Wnt and Notch signaling regulate cerebellum development, and several genes belonging to these pathways are frequently mutated or deregulated in human MBs (see table 1).

Gene product	Genetic or epigenetic change	Frequency (%)
Chromosome 17p loss		**Overall up to 50**
REN	Deletion or reduced expression	39/80
p53	Deletion or mutation	50/<10
Mnt	Deletion or reduced expression	36/42
HIC1	Deletion or reduced expression	42
Hedgehog pathway		**Overall mutations 22.7**
Ptch1	Loss of heterozygosity or mutation	12.8/10
Ptch2	Mutation	0.8
Smo	Mutation	3.3
SUFU	Mutation (+ loss of heterozygosity)	8.6
Gli1	Overexpression	63
Wnt pathway		**Overall: <15**
β-Catenin	Mutation	<10
Adenomatous polyposis	Mutation	<5
Axin1	Mutation	rare
Notch pathway		
Notch1 and Notch2	Overexpression or amplification	12–85/15
HES1–HES5	Overexpression	46–71
ErbB pathway		
ErbB2	Overexpression	40–54
ErbB4	Overexpression or alternative splicing	52–60
Other pathways		
TrkC	Overexpression	40–75
N-myc or Myc	Overexpression or amplification	10–50/5–9
Bmi1	Overexpression	60
Otx2	Overexpression or amplification	63/19
HMGA1	Overexpression	23
PDGFRα	Overexpression	83
IGF2	Overexpression	64

Table 1. Genes frequently mutated or deregulated in human MB tumors.
The most common MB-associated genetic lesion is the loss of chromosome 17p region, associated to deletion or deregulation of the indicated genes. Several genes belonging to the Shh, Wnt and Notch pathway are frequently deregulated or mutated in MB tumors. Of note: Notch1 was undetectable in 40% of cases whereas Notch2 reported overexpressed and amplified; OTX2 was reported overexpressed in 90% of anaplastic MBs; PDGFRα overexpression reported 83% only in metastatic cases, no overexpression was detected in non-metastatic (**adapted from Ferretti e et al. 2005).**

Expression deregulation of several other genes has been also reported in MBs: for example MYCC overexpression is observed in 30% to 50% of tumors and often associated to anaplasia (Stearns et al., 2006). Similarly, expression of the tyrosine kinase receptor ERBB2 has been demonstrated in 40% of MB and more frequently in LCA variants (Gajjar et al., 2004); and the OTX2 transcription factor and the Insulin growth factor receptor-1 (IGF-1R) protein are also over-expressed in most MBs (de Bont et al., 2008; de Haas et al., 2006).

Comparative genomic hybridization (CGH) analyses identified several chromosomal aberrations in medulloblastomas: the most common is loss of the chromosome 17p region, frequently associated with a gain of chromosome 17q, leading to an isochromosome 17q. Both loss of 17p and gain of 17q are prognostically unfavorable factors (Ferretti et al., 2005). Amplification of the MYCC oncogene has been also reported in approximately 5% to 10 % of medulloblastomas and mostly associated with the LCA variant (Eberhart et al., 2004).

The signaling pathways involved in MB tumorigenesis have been also demonstrated, in same cases, attractive therapeutic targets. Indeed, Notch signaling blockade by using pharmacologic inhibitors of gamma secretase, caused induction of differentiation and apoptosis in MB cells, also impairing soft agar colony formation and xenograft tumor growth (Fan et al., 2006; Fan et al., 2004). Similarly, pharmacologic inhibition of the Shh pathway blocked proliferation and induced neuronal differentiation and cell death in MB cells (Berman et al., 2002). Moreover, administration of Shh antagonists was reported to eliminate tumor growth in a mouse model of spontaneous medulloblastoma (Romer et al., 2004).

Emerging evidences indicated that a class of small non-coding RNA, microRNAs (miRNAs) is also involved in MB tumorigenesis.

miRNA expression profiling showed that many of them are aberrantly expressed in primary human MBs tumors (Ferretti et al., 2009), and remarkably, expression of miRNAs that specifically target the Shh or Notch pathways, recapitulated the biological effects mediated by pharmacological inhibition of these signaling (Ferretti et al., 2008; Garzia et al., 2009).

Indeed, we have recently described an oncosuppressor miRNA (miR199b-5p), which targets the Hes1 gene, a key effector of the Notch pathway, and inhibits survival of MB cells also impairing MB cancer stem cell population (Garzia et al., 2009).

Moreover, Ferretti and colleagues described three other miRNAs, miR125b, miR324-5p and miR326, which impair MB cell growth by targeting the Shh pathway (Ferretti et al., 2008).

These findings indicate miRNAs as potential new therapeutic tools for MB treatment.

.

The Sonic Hedgehog (Shh) pathway

The hedgehog signaling, in mammalas, initiates by one of three homologues of the Drosophila hedgehog protein sonic hedgehog (Shh), indian hedgehog (Ihh) and desert hedgehog (Dhh). Among the three Hh family members, Shh is the most broadly expressed and is involved in the patterning and growth of a large variety of organs, including the brain, lung, and skeletal system.

Shh signaling regulates multiple aspects of central nervous system (CNS) development, controlling both cell proliferation and differentiation.

In the developing cerebellum, Purkinje cells secrete Shh, which acts as potent mitogen for GNPs (Fuccillo et al., 2006).

Shh triggers cellular signals by interacting with the 12-pass transmembrane receptor Patched (Ptc). This interaction prevents inhibition of 7-pass transmembrane Smoothened (Smo) co-receptor by Ptc and enables it to activate downstream transcription factors belonging to the Gli family (Gli1, -2 and –3); these factors translocate into the nucleus and activate the expression of target genes such as Gli1 and Ptc themselves, but also important regulators of the cell cycle and apoptosis including N-myc, cMyc, cyclin D1 and D2, Hes1 and Bcl2 gene (Ferretti et al., 2005) (see Fig.2).

Shh signaling was first implicated in MB formation following the discovery of inactivating PTC1 mutations in the germ line of kindred with the nevoid basal-cell carcinoma syndrome (NBCCS, also known as Gorlin syndrome). Patients with NBCCS develop characteristic bone cysts and multiple basal cell carcinomas, and are predisposed to a variety of other tumor types, including medulloblastomas. In mice, heterozygous mutation of PTC1 gene is associated with a 15% of incidence of MB over a period of 10 months (Goodrich et al., 1997). Moreover, the lack of p53 in PTC1 heterozygous mice increases the incidence of MB to >95% also decreasing the latency over a period of 12 weeks (Wetmore et al., 2001). These mouse tumors display a very similar gene expression

signature to those of human PTC1 mutant tumors, both showing induction of Shh target genes. Among them, Gli1 is an important effector of Hedgehog-induced tumorigenesis, as inactivation of both Gli1 alleles in PTC1 heterozygous mice significantly reduces MB formation (Kimura et al., 2005).

Remarkably, suppression of the Shh pathway by using small molecule inhibitors, arrests MB formation in PTC-/+ as well as PTC-/+ p53-/- mice (Berman et al., 2002; Romer et al., 2004). For these reasons inhibition of the Shh pathway can be an effective treatment for MB tumors.
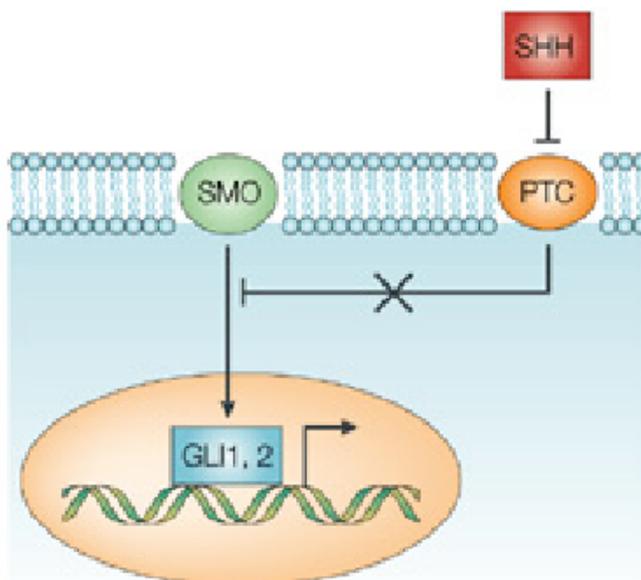
Figure 2. Diagram of the Shh pathway. *In the absence of the Shh ligand, Ptc represses Smo. Signaling is initiated by binding of Shh to Ptc, which relieves the repression of Smo. Subsequently, Smo signals to the nucleus by increasing the concentration of Gli transcription factors, which recruit co-activators to activate downstream target genes.* **From (Radtke and Ray, 2003)**

The Notch pathway

The Notch pathway is evolutionarily conserved and presents in organisms as diverse as worm and humans. Humans express four different Notch receptors (Notch1 -4), which are homologous of the drosophila receptor dNotch, and five drosophila Delta and Serrate homologues ligands, named Delta-like-protein 1 –3 and –4 (DLL1, DLL3 and DLL4) and Jagged 1 and Jagged 2 (Jag1 and Jag2) (see Fig.3).

The ligands share several characteristics with the Notch receptors: both are expressed as transmembrane proteins, with large N-terminal extra-cellular portions consisting of varying numbers of EGF-like repeats (Fig.1) (Radtke & Raj, 2003).
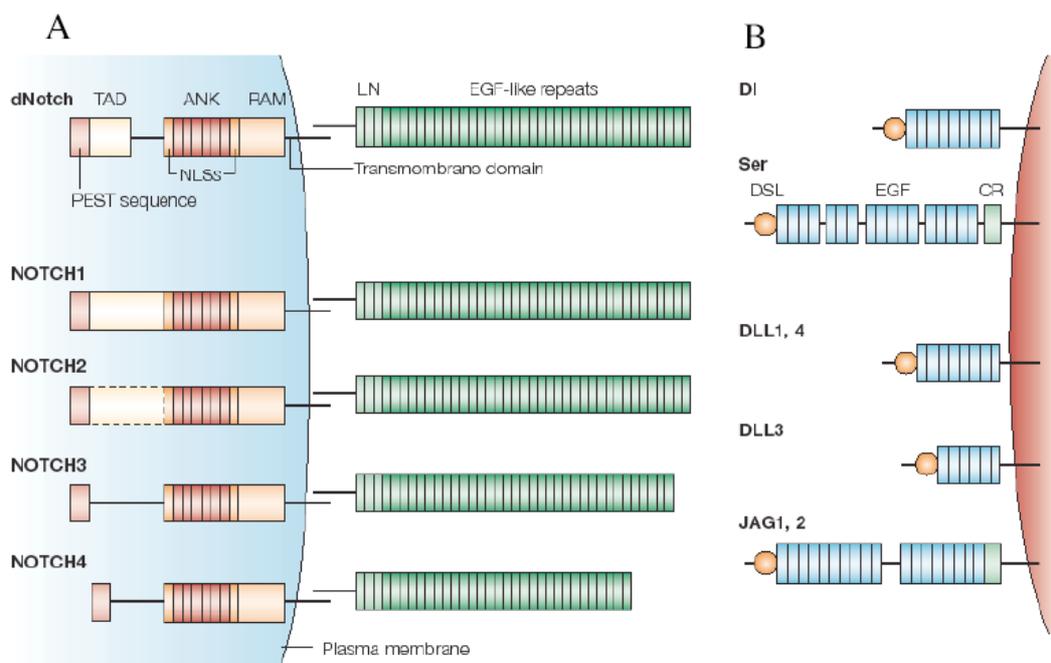
Figure 3. Structure of Notch receptors and ligands. *A*. *Drosophila has one Notch receptor (dNotch) and vertebrates have four (Notch1-4), which are presented on the cell surface as heterodimers. The extracellular domain contains epidermal-growth-factor (EGF)-like repeats and a cystein-rich Notch/Lin12 domain (LN); this is followed by the transmembrane domain, the RAM domain and six ankyrin repeats (ANK), two nuclear localization signals (NLSs), followed by the transactivation domain (TAD) and a PEST sequence*. *B*. *Two transmembrane-bound ligands for Notch have been identified in Drosophila, named Delta (Dl) and Serrate (Ser). The vertebrates possess three Delta-like ligands (DLL) –1, -3, 4, and two serrate homologues, Jagged 1 (JAG1) and Jagged 2 (JAG2). The ligands harbour an amino terminal structure called DSL (Delta, Serrate and LAG-2), which is common to all family members, followed by EGF-like repeats. Serrate, Jagged1 and Jagged2 harbour a cysteine-rich domain (CR following the EGF-like repeats.* **Adapted from (Radtke & Raj, 2003).**

Ligand-receptor interaction take place between two neighboring cells and results in two successive proteolitic cleavages at the transmembrane portion of the Notch receptor. Two transmembrane enzymes, the ADAM10 or TACE (TNF-a-converting enzyme) metalloprotease and the γ-secretase complex, mediate the receptor processing, which results in the release of the Notch intracellular domain (NICD) from the membrane (see Fig.4). NICD subsequently enters the nucleus and binds to the transcription factor CSL (CBF1, Su(H) and LAG1). Through interaction with NICD, CSL is converted from a repressor into an activator of transcription and induces expression of the Notch target genes. One of the best-characterized targets is the HES (hairy/enhancer of split) family of transcription factors, which consists of Hes1, -3 and –5, all negative regulators of gene expression (Radtke & Raj, 2003).
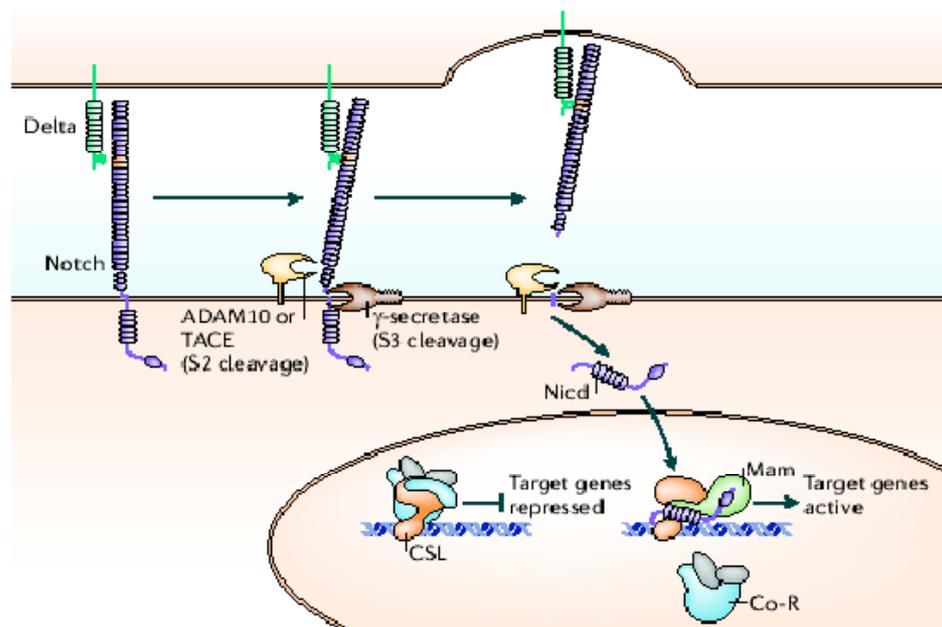
Figure 4. The Notch pathway. *Binding of the Delta (green) on one cell to the Notch receptor (purple) on another cell results in two proteolytic cleavages of the receptor. The ADAM10 or TACE (TNF-α-converting enzyme) metalloprotease (yellow) catalyses the S2 cleavage, generating a substrate for S3 cleavage by the γ-secretase complex (brown). This proteolytic processing mediates release of the Notch intracellular domain (Nicd), which enters the nucleus and interacts with the DNA-binding CSL (CBF1, Su(H) and LAG-1) protein (orange). The co-activator Mastermind (Mam;green) and other transcription factors are recruited to CSL complex, whereas co-repressors (Co-R; blue and grey) are released.* **From (Bray, 2006).**

Besides activating the Notch receptors via cell-cell interactions, Notch-ligands can cell autonomously antagonize Notch signaling (Ladi et al., 2005). DLL ligands cell autonomously bind Notch1 receptor. This complex is not present on the cell surface but retained in the endoreticulum or Golgi apparatus. DLL-Notch cell autonomous interaction show a dominant negative effect interfering with the ability of the cell to receive Notch signal by neighboring cells (Sakamoto et al., 2002).

The Notch pathway is involved in the development of several organs, including the nervous system. In particular the Notch pathway is required for the correct neuronal and glial differentiation of the cerebellum, and for the proliferation of GNPs and NSCs (Louvi & Artavanis-Tsakonas, 2006).

Notch1 and Notch2 receptors have distinct roles in controlling proliferation and differentiation of GNP cells: Notch2 signaling acts as a mitogen for cerebellar GNPs, whereas Notch1 receptor is only expressed in differentiated granule neurons and is not detected in proliferating precursor cells (Fan et al., 2004; Solecki et al., 2001). Differential expression of Notch1 and Nocth2 receptors was also detected in human MB tumors with Notch2 over-expressed, and Notch1 mRNA detected at very low levels (Fan et al., 2004). Also, Hes1 expression is associated with decreased survival rate of MB patients (de Bont et al., 2008), and interestingly, is induced upon Notch2, but not Notch1 activation, in MB cells (Fan et al., 2004). In vitro studies indicate that Notch1 and Notch2 receptors have opposite effects in MB cells: Notch2 activation promotes cell proliferation, soft agar colony formation and xenograft growth, whereas Notch1 activation induces apoptosis (Fan et al., 2004). Consistently, MB cells show constitutive activation of Notch2 whereas Notch1 is inhibited (Fan et al., 2004), therefore Notch signaling blockade, by using γ-secretase inhibitors, causes cell cycle exit, apoptosis and differentiation in MB cells (Fan et al., 2006), thus effects only referable to the Notch2 signaling inhibition.

For these reasons the Notch signaling is considered an important therapeutic target for MB treatment.

Small non protein-coding RNAs: microRNA (miRNA)

Biogenesis

MicroRNAs (miRNAs) are small non-coding RNAs able to post-trascriprionally regulate gene expression through translational inhibition and destabilization of their target mRNAs. Almost one thousand of human miRNAs have been identified and are predicted to regulate about one third of human genes (Pillai et al., 2007).

miRNAs map either within interegenic regions, as independent transcription units, or into introns or exons of protein-encoding genes, coexpressed with the host gene or independently transcribed via alternative promoters. They can be expressed as single transcription units or clustered within policistronic transcripts (see Fig.5) (Baskerville & Bartel, 2005; Rodriguez et al., 2004).

miRNAs are transcribed as very long primary transcripts (pri-miRNAs) by RNA polymerase II (Lee et al., 2004) or RNA polymerase III (Borchert et al., 2006).

Pri-miRNAs are usually several kilobases in length and, like protein coding mRNAs, are 7-methyl guanosine capped at the 5' end, and polyadenylated at the 3' end (Lee et al., 2004). Each miRNA sequence folds as imperfect hairpin-like stem loop structures of ≈ 3 helical turns. These structures are recognized and processed by a protein complex called "Microprocessor" consisting of Drosha, an RNAse III enzyme and its cofactor DGCR8 (Lee et al., 2003). Drosha transiently interacts with the stem region of the hairpin and cleaves the RNA duplex about 11 nt from the double strand region (SD junction) (Han et al., 2006).

The Drosha-mediated processing of pri-miRNAs occurs co-transcriptionally and generates 70nt precursor miRNAs (pre-miRNA), containing a 2-nt overhang at its 3' end (Lee et al., 2003; Morlando et al., 2008).

pre-miRNAs are exported outside the nucleus by the nuclear transport factor exportin-5 (Exp5) (Lund et al., 2004) and, once in the cytoplasm, are processed by the RNase III

enzyme Dicer, as part of a complex including also TRBP and Argonaute 2 (Ago2) proteins (see Fig.5) (Diederichs & Haber, 2007). Dicer recognizes the double stranded portion of the pre-miRNA and cuts both strands of the duplex, at about two helical turns away from the base of the stem loop. This processing generates an imperfect duplex of 19 nt, and 2-nt unpaired overhangs at each 3'-end, and a 5'- phosphate on each strand (Standart & Jackson, 2007).

The duplex is unwound, by a helicase which is still unknown, resulting in the release of two single-strand RNAs: the mature miRNA, generally selected as the duplex strand with the thermodynamically less-stable 5' end, which is loaded into a multi protein complex known as RNA-induced silencing complex (RISC); and the mature miRNA-complementary strand, known as miRNA "star" (miRNA *), which is rapidly degraded (Bartel, 2004; Khvorova et al., 2003).

The mature miRNA-RISC ribonucleoprotein complex can then regulates the expression of miRNA target genes by inducing mRNA degradation or translational repression, through different proposed mechanisms (see Fig.5).
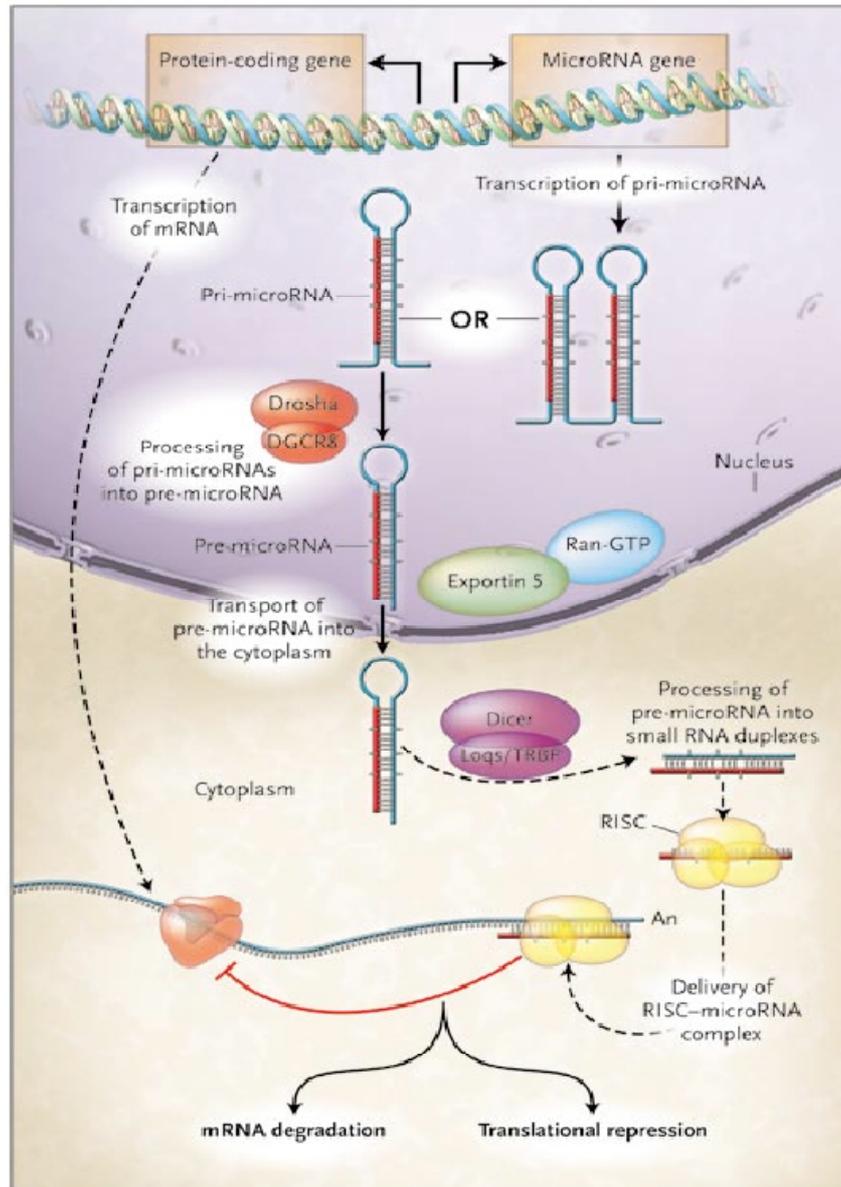
Figure 5. miRNA biogenesis. *Single or clustered miRNAs are transcribed as pri-miRNAs and fold as hairpin-like structures. Drosha cleavage generates a precursor miRNA (pre-miRNA) which is exported outside the nucleus by the nuclear factor exportin-5. Dicer processes pre-miRNAs within the cytoplasm and generates the 21-nt duplex, which contains the mature miRNA sequence. The RISC complex loads the mature miRNA and, upon miRNA/mRNA pairing, regulates target mRNA expression by inducing mRNA degradation or translation inhibition.* **From (Chang-Zheng C., 2005).**

Mechanisms of action of miRNAs

The last step of miRNA maturation results in the formation of the 21nt-mature miRNA, which is loaded within the RISC complex.

RISC is a multi protein complex consisting of several subunits including Argonaute (Ago) proteins and GW182, an RNA binding protein. Ago proteins are a large family of 95 Kda proteins consisting, in mammals, of four members (Ago1 to Ago4) that directly bind miRNAs. Among them, Ago2 has Rnase H enzymatic activity (Filipowicz et al., 2008).

miRNAs pair complementary sites (miRNA binding sites) within the mRNA target sequences, allowing the RISC complex to be loaded on the target mRNA.

Target recognition represents an important step for miRNA functions, as it confers selectivity and efficacy of action.

In most reported cases animal miRNAs pair through imperfect complementarity with their binding sites residing within the 3'UTRs (3' untraslated regions) of target mRNAs. However emerging evidences demonstrated that 5' UTRs and open reading frames (ORFs) of several genes can contain miRNA-binding sites and thereby can be recipients of the miRNAs activity (Lytle et al., 2007; Tay et al., 2008).

Several features of both miRNA and mRNA sequences determine the specificity and the efficacy of the binding.

1) Perfect pairing between the miRNA seed region (2-7 nt of the 5' end) and miRNA binding site within the target 3'UTR revealed in some cases sufficient for target downregulation (Brennecke et al., 2005). However, seed sites do not always confer repression, and when repression occurs, the degree of repression is highly variable in different UTR contexts. Supplemental pairing outside of the seed region, particularly to nucleotides 13-16 of the miRNA, can indeed increase the repression efficiency (see Fig.6) (Grimson et al., 2007).

2) Multiple miRNA binding sites within the same 3'UTR have shown multiplicative effects in mRNA destabilization, moreover a greater repression was observed when the miRNA-binding sites were close each other (Grimson et al., 2007).

3) miRNA binding sites are fully functional only in their endogenous positions within the targeted UTR, and mutations of the flanking regions also impair miRNA functions suggesting that they could represent protein binding sites or provide an appropriate structural context (Didiano & Hobert, 2008). Moreover AU-rich nucleotide composition immediately flanking the miRNA binding sites, increases their efficacy as functional site (Grimson et al., 2007).
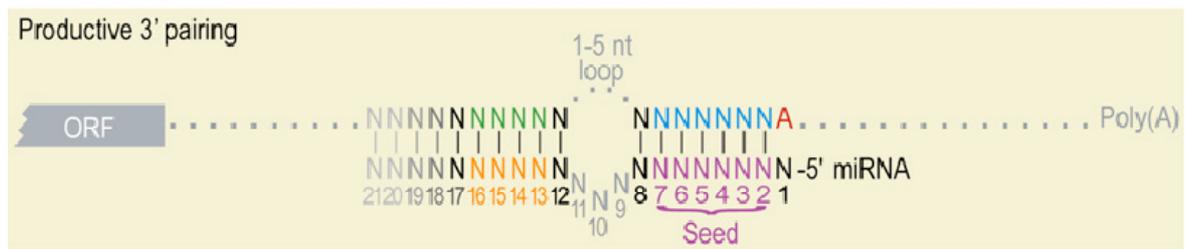
Figure 6. Characteristics of miRNA/mRNA pairing. *Pairing scheme, of a productive 3' pairing by imperfect complementarity between the miRNA and 3'UTR. Perfect pairing between the 2-7nt seed sequence (purple) of the miRNA and the complementary sequence of the target 3'UTR (blue) is necessary for a productive interaction. Moreover, supplemental pairing to nucleotides 13-16 (orange) of the miRNA increases the binding affinity. The bulge presents in the central region of the miRNA-mRNA duplex precludes the Ago2-mediated endonucleolytic cleavage of the mRNA.* **From: (Grimson et al., 2007).**

miRNA/mRNA binding features also determine the fate of the target mRNA. Indeed, perfect miRNA/mRNA pairing preferentially induces target mRNA cleavage, as is the case of most plant miRNAs, whereas partial miRNA/mRNA complementarity (depicted in Fig.6), observed in the majority of animal miRNAs, can lead to both translational repression or accelerated decay of the target mRNA (Kiriakidou et al., 2007).

Indeed, numerous studies, often coming to divergent results, have provided experimental evidences that miRNAs can either repress translation of endogenous mRNAs or artificial reporters, without affecting the target mRNA levels (Mathonnet et al., 2007), or induce deadenylation and subsequent decay of target mRNAs (Eulalio et al., 2009; Wu et al., 2006).

The translational inhibition was reported to occur to either the initiation or post-initiation step, or even both, depending on the miRNA, the cellular context and the experimental procedures employed (see Fig.7).

One proposed mechanism by which miRNAs can inhibit initiation of translation relies on the capacity of Ago2 protein to bind the 7-methyl cap (m7G cap) to the target mRNAs 5' end (Kiriakidou et al., 2007). Thus, Ago2 can displace the translational initiation complex from the binding of the m7G cap and interferes with the initiation of translation. Several other experimental evidences support such mechanism of action. Indeed, cap-independent translation of reporter mRNAs bearing internal ribosome entry site (IRES) elements failed to be repressed in several reports, and in cell free systems the m7G-cap was required for miRNA repression (Humphreys et al., 2005; Mathonnet et al., 2007; Wakiyama et al., 2007). In other studies miRNAs functions required also an intact poly(A) tail and translational repression only occurred when target mRNAs contained both an m7G cap and the poly(A) tail (Wakiyama et al., 2007). Other studies, in Hek293 cell extracts, showed that mRNAs containing miRNA-binding sites underwent deadenilation irrespective of whether they contained an m7G cap or IRES sequences.

miRNA-mediated deadenilation might then decrease the stability of mRNAs and inhibit translation by disrupting the mRNA circularization, which is required to increase translation efficiency (Eulalio et al., 2009; Wakiyama et al., 2007; Wu et al., 2006).

Other studies have proposed additional mechanisms of translation inhibition, by which the miRNA-RISC complex can physically interfere with either the ribosomal subunits recruitment to the target mRNA or the translation elongation process, rendering ribosomes

prone to premature termination of translation (see Fig.7) (Lytle et al., 2007; Wu L and Belasco, 2008). Possible cotraslational degradation of nascent peptides induced by miRNAs has been also proposed, however the involved protease enzyme is yet to be identified. The proposed miRNA mechanisms of action are depicted in Fig.7.

Significant fractions of miRNA-repressed mRNAs are found concentrated in cytoplasmic foci known as p-bodies (processing bodies). P-bodies are dynamic aggregates of RNA and proteins containing high concentrations of miRNAs and RISC-associated proteins (Ago 1-4, GW182, etc.) but lack ribosomes and all translation initiation factors, with the exception of eIF4E (Pillai et al., 2007). However, whether the P-bodies actively contributes to the translational inhibition mediated by miRNAs is still unclear (Wu & Belasco, 2008).

Of note, Vasudevan and colleagues have recently shown that miRNAs are able to stimulate the translation of target genes during cell cycle arrest conditions (Vasudevan & Steitz, 2007; Vasudevan et al., 2007). This effect involves the recruitment of the RNA binding protein FXR1 to the miRNA-Ago complex. However the mechanisms by which miRNAs enhance translation, and who are the other players of this intriguing function remains still unknown.
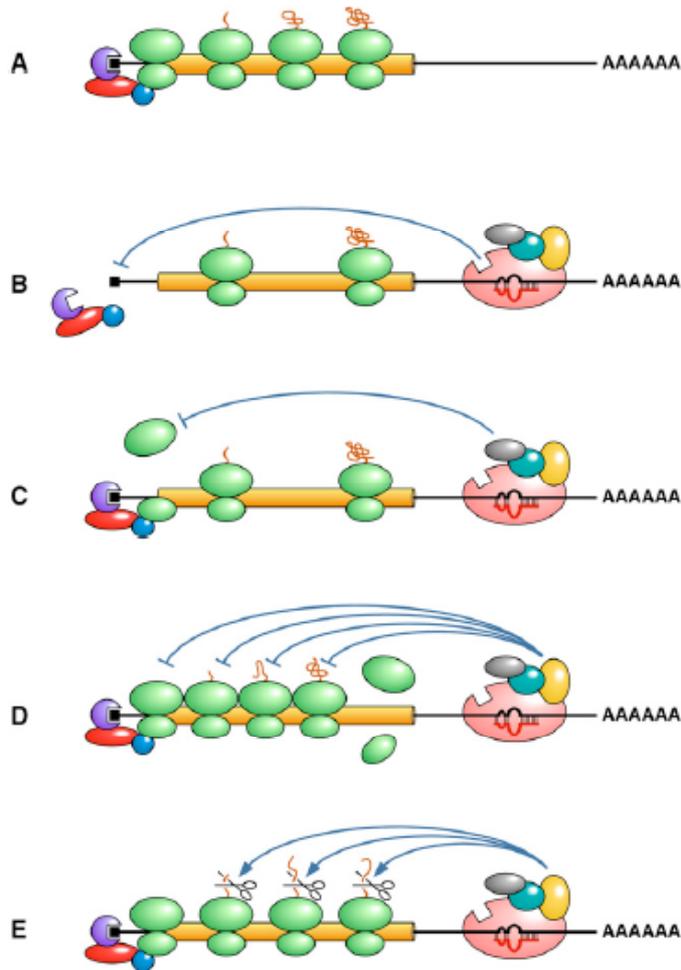
Figure 7. Proposed mechanisms of translational repression by miRNAs. (A) *mRNA undergoing translation in the absence of a bound miRNA. Black square, m7G cap; amber cylinder, protein-coding region; and AAAAAA, poly (A) tail. Ribosomes are colored green, nascent polypeptides are brown, and the eIF4E subunit of the cap-binding complex is violet. (B) Inhibition of translation initiation by competition between RISC and eIF4E for cap binding. RISC is depicted as a ribonucleoprotein complex comprising a miRNA (red), Ago (pink), and other protein subunits. (C) Inhibition of translation initiation at a step after cap recognition, such as by impeding the association of the small and large ribosomal subunits. (D) Inhibition of translation elongation coupled to premature termination. (E) Cotraslational degradation of nascent polypeptides.* **From (Wu L and Belasco, 2008).**

miRNAs and cancer

Although computational approaches have identified almost one thousand of miRNAs mapping everywhere within the human genome, only a few of them have been experimentally validated and functionally characterized (Pillai et al., 2007).

Bioinformatics analyses indicate that more than 30% of protein–coding genes may be targeted by miRNAs, and each miRNA can recognize dozens of targets (Lewis et al., 2005). Hence, not surprisingly, several reports indicate that miRNAs are involved in virtually every biological process, including proliferation, differentiation and apoptosis (Miska, 2005).

Indeed, loss of Dicer leads to lethality early in embryogenesis, with dicer-null embryos depleted of stem cells (Bernstein et al., 2003) and knock out mice, with loss of the cluster miR17-92 die shortly after birth, showing lung hypoplasia and ventricular septal defects (Ventura et al., 2008).

Interestingly, more than 50% of miRNA genes are located in cancer-associated genomic regions or in fragile sites (Calin et al., 2004) and mutations and miss-expression of miRNAs have been correlated to various tumors (Calin & Croce, 2006).

To date, several lines of evidences indicate that miRNAs are directly involved in the tumorigenesis of many cancers.

For example, Dr Takamizawa and colleagues observed that the expression levels of the miRNA let-7 were frequently reduced in lung cancers and that reduced expression of let-7 significantly associated with shortened postoperative survival (Takamizawa et al., 2004). Moreover they reported that over-expression of let-7 in lung cancer cell lines inhibited tumor cell growth.

As the let-7 gene, several other miRNAs have been classified as oncogenes or oncosuppressors according to their functions in cellular trasformation. Hence, miRNAs

have been proposed as potential tools for diagnosis, prognosis and therapy of many cancers (Zhang et al., 2007).

The molecular mechanisms by which miRNAs can regulate tumorigenesis are unclear. One possible mechanism is that miRNAs regulate cancer pathogenesis by targeting oncogenes and/or oncosuppressor genes. We recently provided evidences that support this mechanism in the MB tumors. Indeed, we have recently shown that miR199b-5p, through direct targeting of Hes1 gene, key effector of the Notch pathway, exerts onco-suppressor functions in MB cells. We reported that over-expression of miR199b-5p impairs proliferation of different MB cells and affects survival of the MB stem-cell subpopulation (Garzia et al., 2009).

Ferretti and colleagues, also reported oncosuppressor effects mediated by miRNAs in MB cells, showing that miR125b, miR324-5p and miR326 inhibit cell growth by targeting Smo or Gli1 gene, two crucial effectors of the Shh pathway (Ferretti et al., 2008).

Although the biological functions of miRNAs in the MB tumor context have been just discovering, these findings indicate that miRNAs are important regulators of MB tumorigenesis.

miR34a

miR34 is an evolutionary conserved family of miRNAs consisting of three members in vertebrates (miR34a, miR34b and miR34c), and one orthologue in invertebrates species.

In human, miR34a precursor sequence maps within the second exon of a EST (expressed sequence tag) within the chromosome 1p36.23; on the other hand, miR34b and miR34c are located within the intron 1 and exon 2, respectively, of the same EST within the chromosome 11q23.1.

Several groups have recently reported that the three miR34 family members are direct targets of p53 transcription factor (He et al., 2007; Corney et al., 2007; Bommer et al., 2007); in particular, miRNA expression profiles of five different studies reported miR34a as the most significantly induced miRNA after activation of p53 (Chang et al., 2007; He et al., 2007; Raver-Shapira et al., 2007; Tarasov et al., 2007; Tazawa et al., 2007).

p53 binding sites were identified 30Kb upstream of the mature miR34a and 3kb upstream of the cluster miR34b/c (Corney et al., 2007; Raver-Shapira et al., 2007), and chromatin immunoprecipitation analyses confirmed the p53 binding (Bommer et al., 2007; He et al., 2007; Raver-Shapira et al., 2007; Tarasov et al., 2007).

Interestingly, ectopic expression of miR34a recapitulated p53 mediated effects including cell cycle arrest (Bommer et al., 2007; He et al., 2007; Raver-Shapira et al., 2007; Tarasov et al., 2007) and induction of apoptosis (Chang et al., 2007; Raver-Shapira et al., 2007; Tarasov et al., 2007; Welch et al., 2007) and senescence-like phenotype (He et al., 2007; Tarasov et al., 2007). Remarkably, inhibition of miR34a functions via miR34a-specific LNA (locked nucleotide analogs) impaired p53-induced apoptosis, upon DNA damage induction (Raver-Shapira et al., 2007). Therefore, miR34a can be, in some cases, not only sufficient but also required for mediation of tumor suppression by p53.

Of note Dr Dutta and colleagues showed that miR34a-mediated effects can be cell-type dependent, since it also supports cell proliferation of HeLa and MCF-7 cells (Dutta et al., 2007).

To date, several miR34a targets have been experimentally validated, including CDK4/6, cyclin E2, cyclin D1, E2F5, MET, Bcl2, MYCN and SIRT1 (Bommer et al., 2007; He et al., 2007; Sun et al., 2008; Tazawa et al., 2007; Wei et al., 2008; Yamakuchi et al., 2008).

Interestingly, SIRT1 gene (silent information regulator 1) inactivates p53 by deacetylating it (Yamakuchi et al., 2008), thereby generating a positive feedback loop in which p53 regulates miR34a, which through SIRT1, increases p53 activity. In agreement with this observation, two different research groups reported that miR34a induction of apoptosis observed in p53-wt HCT116 cells was strongly attenuated in p53-knock out HCT116 cells (Chang et al., 2007; Yamakuchi et al., 2008).

miR34a expression was reported significantly downregulated in several human cancers, and aberrant CpG methylation of its promoter was observed in prostate carcinomas and primary melanomas, as well as in several tumor cell lines, including lung, breast and colon carcinoma cell lines (Lodygin et al., 2008).

The high similarity among the three processed miR34 family members suggested that they may have the same targets. Indeed, after separate transfection of miR34a, miR34b and miR34c the affected mRNAs were almost identical (He et al., 2007) and although most of the functional studies focused on oncosuppressor activities of miR34a, the ectopic expression of miR34b and miR34c was also reported to induce cell cycle arrest and cellular senescence-like phenotype in tumor cell lines (He et al., 2007). miR34b was also found silenced by hypermethilation of its promoter in oral squamous cell carcinomas (Kozaki et al., 2008). However, miR34a and the cluster miR34b/c have distinct tissue-specific expression patterns, with miR34a presents at highest levels in the mouse brain, and low or moderate levels in other tissues, whereas miR34b and miR34c most highly expressed in lung (Bommer et al., 2007).

In particular, in situ hybridization analysis of rat organs showed the highest expression of miR34a within the cerebellum cortex, thus suggesting potential biologic roles of the endogenous miRNA in this brain tissue (Dutta et al., 2007)

MATERIALS AND METHODS

Cloning vectors

The miR34a sequence was HindIII/XhoI cloned into a pCDNA3 vector. The seed mutant was made by site-directed mutagenesis, using the pfu enzyme according to manufacturer protocol (Roche). The GGC sequence at the seed positions 2-4 of miR34a was replaced with AAA.

The 620 nt genomic region consisting of miR34b and miR34c precursor sequences and about 400 nt of spacing genomic region, was HindIII/XhoI cloned in pCDNA3 vector. The seed mutants were made as for miR34a.

The full-length 3'-UTR of target genes were Not1-cloned into a pRL-CMV vector (PROMEGA) downstream of the Renilla luciferase coding sequence. The mutant of DLL1-3'UTR reporter construct was generated by site-directed mutagenesis as above. The TGCC sequence within the three miR34a-binding sites was replaced with AAAA. The oligonucleotides sequences of primers pairs employed for vector cloning are shown in table 2. All of the vectors produced were sequence verified.

The CSL transcription factor reporter construct and the NICD1 expressing vector were a kind gift of Prof. Nicola Zambrano, University Federico II, Naples. Murine DLL1 expressing construct was a kind gift of Dr Shigeru Chiba department of Cell Therapy and Transplantation Medicine University of Tokyo Hospital, 7-3-1 Hongo, Bunkyo-ku, Tokyo 113-8655, Japan.

A pool of three Sh-RNA expressing constructs targeting DLL1 was used in our transfections (clones ID: V2HS_56928; V2HS_56927; V2HS_56930) (Openbiosystems, 601 Genome Way Ste. 2100 Huntsville, AL 35806).

Notch1UTRs	AAAAGCGGCCGCTCCTTTCCCAAGCCTTCGG
Notch1UTRas	AAAAGCGGCCGCAAATCAACATCTTGGGACGC
Notch2UTRs:	AAAAGCGGCCGCGAGAGTCCACCTCCAGTG
Notch2UTRas:	AAAAGCGGCCGCTAGTGCACAGAAGAGTGCTC
GLI1UTRs:	AAAAGCGGCCGCAGAGTAGGGAATCTCATCC
GLI1UTRas	AAAAGCGGCCGCGCAGTTCCTTTATTATCAGG
DLL1UTRs:	AAAAGCGGCCGCGTGAGATGGCAAGACTCC
DLLUTRas:	AAAAGCGGCCGCACATAGACCCGAAGTGCC
Jag1UTRs	AAAAGCGGCCGCGTACATCGTATAGCAGACCG
Jag1UTRAs	AAAAGCGGCCGCAGTTCCAGCTTCACAGCAG
miR34aHINDse:	AAAAAAGCTTGGCCAGCTGTGAGTGTTTC
miR34aXhoAS:	AAAACTCGAGGCTTCATCTTCCCTCTTGG
miR34b/c prHind S	AAAAAAGCTTGTGCTCGGTTTGTAGGCAG
miR34b/c prXho AS	AAAACTCGAGCACATTGATGATGCACAGGC
SeedM34aS:	CTGTGAGTGTTTCTTTAAAAGTGTCTTAGCTGGTTG
SeedM34aAS:	CAACCAGCTAAGACACTTTTAAAGAAACACTCACAG
SeedMmiR34b S	GCTTGTGCTCGGTTTGTAAAAAGTGTCATTAGCTG
SeedMmiR34b AS	CAGCTAATGACACTTTTTACAAACCGAGCACAAGC
SeedMmiR34c S	GAGTCTAGTTACTAAAAGTGTAGTTAGCTG
SeedMmiR34c AS	CAGCTAACTACACTTTTTAGTAACTAGACTC
3'UTR DLL1 Mut site1S	GGCCGCCTGCGGCACAAAATTCCGTGACGTCGC
3'UTR DLL1 Mut site 1AS	GCGACGTCACGGAATTTTGTGCCGCAGGCGGCC
3'UTR DLL1 Mut site 2S	ATAAGAAGCATGCACAAAATGAGTGTATATTTG
3'UTR DLL1 Mut site 2AS	CAAAATATACACTCATTTTGTGCATGCTTCTTAT
3'UTR DLL1 Mut site 3S	TAGAAACACAAACACAAAATTTATTGTCCTTTTT
3'UTR DLL1 Mut site 3AS	AAAAAGGACAATAAATTTTGTGTTTGTGTTTCTA

Table 2. Oligonucleotides developed as primer-pairs used for cloning.

miRNA target prediction databases used in this study

MiRanda: http://microrna.sanger.ac.uk/sequences;

TargetScan: http://genes.mit.edu/targetscan;

PicTar: http://pictar.bio.nyu.edu;

PITA: http://genie.weizmann.ac.il/pubs/mir07/mir07_prediction.html.

Cell culturing

Daoy and D283-MED medulloblastoma cells were maintained in Eagle's Minimum Essential Medium (Eagle's MEM, Sigma Aldrich, Milan, Italy); ONS76 medulloblastoma cells were cultured in RPMI medium; SH-SY5Y, SK-N-BE, and GIMEN neuroblastoma cells, and MCF7 and MDA 231 human breast cancer cells were maintained in DMEM medium (Sigma Aldrich, Milan, Italy). All media were supplemented with 10% fetal bovine serum (Celbio Pero, Milan, Italy), 10 U/ml penicillin and 0.1 mg/ml streptomycin (Celbio Pero, Milan, Italy).

Stable clone selection

Daoy cells were transfected by using *Trans*IT-LT1 reagent (Mirus) according to manufacturer instructions. Briefly, cells were plated in 10 cm dish plates at a 60% confluence. The following day, the cell culture medium was replaced 16 ml of complete growth medium and a mix of 45ul *Trans*IT-LT1 reagent and 15ug of DNA were added to the cells. Upon 48 h cells were maintained in a complete growth medium containing 0.3 µg/ml neomycin (GIBCO). Following almost three weeks single clones (clone#1 and #2) and one mixed clone (clone#3) were selected.

Luciferase assays

In luciferase assays performed in Daoy, SH-Sy5y, SK-N-BE and GIMEN cells, cells were transfected with the indicated reporter constructs and miR34a or seed mutated miR34a expressing vectors or empty vector, by using *Trans*IT-LT1 reagent (Mirus) according to manufacturer instructions. The pGL3 control vector (PROMEGA) was used for transfection normalization. Experiments were performed in triplicate in 96-well plates, and luciferase assays were carried out following 24 h of transfection using the Dual-luciferase Reporter assay system (PROMEGA), according to manufacturer procedures.

For luciferase assays performed HEK293 cells, DNA vector transfectios were performed using $CaCl_2$ and Na_2PO_4 reagents. The pGL3 control vector (PROMEGA) was used for transfection normalization. Experiments were performed in triplicate in 96-well plates, and luciferase assays were carried out following 24 h of transfection using the Dual-luciferase Reporter assay system (PROMEGA), according to manufacturer procedures.

Time-course experiments

Two different transfections were performed in 6-well-plated Daoy and D283-MED cells to obtain the following time points: first transfection, from 6 h to 14 h; second transfection, from 16 h to 20 h. The cells were transfected at a 80% confluence by using *Trans*IT-LT1 reagent (Mirus) using 7 μl of reagent and 2.5 μg of DNA per well. At each time point, the cells were harvested and lysated using RIPA buffer or TRIZOL reagent, according to manufacturer instructions. For western blotting the following antibodies were used: Delta1 (H-265) sc-9102 (Santa Cruz) (≈77 kDa); activated Notch2 (ab8926) (Abcam) (≈82 kDa); Notch1 (ab52627) (Abcam) (≈120 kDa); Hes1 (kind gift of Dr.Tetsuo Sudo, TORAY Industries, Tebiro Kamakura, Japan) (≈35 kDa); ANTI-β-actin (A5441) (SIGMA).

Of note, in the Daoy cell time-course experiments, the DLL1 protein was detected as a clear band of ≈77 kDa (predicted molecular mass), however a band of ≈95 kDa was also

observed when more then 30 μg total lysate was loaded (western blotting of the stable clones). The two bands were both down-regulated by miRNA34a. In D283-MED cells, DLL1 was detected as two clear bands: 77 kDa and 160 kDa, on the same films. Each band was down-regulated at the same rate at the 10h time point.

RT-PCR and real-time PCR detection

Total RNA was extracted and 2 μg were retro-transcribed using the ISCRIPT enzyme (BIORAD), according to manufacturer protocol. Total RNA was extracted from cerebellar controls or tumoral specimens by homogenizing the samples within TRIZOL reagent according manufacturer instructions. RNA was then retro-transcribed as above. Syber-green real-time PCR was performed using standard protocols, with an Applied Biosystems (Foster city, CA) 7900-HT FAST real-time PCR sequence detection system, as described previously (Bulfone et al. 2005). Experiments were performed in duplicate, and human sn-U6 RNA or GAPDH and β-ACTIN were used as references for miR34s or mRNA expression, respectively. The primers were generated by using the Primer Express program, acquired from Applied Biosystems.

MTS cell proliferation assay

For stable clones, viable cells (2,000) were plated in 96-well plates and left over-night. MTS proliferation assay was then performed by using the CellTiter 96[R] AQ$_{ueous}$ One Solution Reagent Non-Radioactive Cell Proliferation Assay (PROMEGA), according to manufacturer procedure. Breafly, upon the indicated time points cell culture medium was replaced with a tetrazolium compound containing complete growth mediun. Upon two hours absorbance at 490nm was measured by using EnVision 2102 multilable reader instrument (PerkinElmer, Waltham, Massachusetts 02451, USA).

For transiently transfected cells, six well-plated cells were transfected as previously described. Upon 24 hours from transfection 2000 viable cells were plated in 96-well plates. MTS was performed as above.

Apoptosis Analysis.

For FACS analysis, 500.000 viable cells of miR34a Daoy stable clones and the empty vector clone were harvested and stained with propidium iodide and anti-Annexin-V antibody. Cells were, subsequently, analyzed by using the FACS Calibur instrument (Becton Dickinson, San Jose CA).

D283-MED and ONS-76 cells plated in 96-well plates were transfected using the *Trans*IT-LT1 reagent (Mirus). After the indicated time, the cells were lysated by adding to the growth medium equal amount of lysis buffer 2X (60 mM Tris, pH 7, 300 mM NaCl, 2% Triton X 100, 2% glycerol). Ten μl lysate was incubated for 1 h at 37 °C in the dark in 96-well plates (CORNING) with 90 μl reaction mix: 10 μl reaction buffer (20 mM Hepes, 10 mM NaCl, 1 mM EDTA, 0.1% CHAPS), 50 μl 20% sucrose, 1 μl 1 M DTT, 0.2 μl fluorigenic caspase 3/7 substrate, 20 mM Ac-DEVD-AFC (BIOMOL), made up to 90 μl with water. After a 1-h incubation in the dark, fluorescence emission at 505nm was detected by using EnVision 2102 multilable reader instrument (PerkinElmer, Waltham, Massachusetts 02451, USA)., at 505 nm emission..

2'-0-Methyl antisense experiments

miR34a-2-0-Methyl antisense is a chemically synthesized, single-stranded, modified RNA which specifically inhibits endogenous miR34a functions after transfection into cells (http://www1.qiagen.com/Products/miScriptmiRNAInhibitors.aspx) (product name: Anti-has-miR-34a) (QIAGEN S.p.A. Via Grosio, 10/10, 20151 Milano). Unrelated-2-O-methyl

antisense was synthesized and chemically modified by Prof Aldo Galeone, University of Naples and Biological Science faculty, Italy.

Oligos were transfected at a final concentration of 80 nM by using *Trans*IT-LT1 reagent (Mirus) according to manufacturer instructions in 96 well or 6 well-plated Daoy cells, for caspase assays or western blots analyses, respectively. Following 8 hours from transfection cell culture medium was replaced with fresh or doxorubicin containing medium (final concentration 0.2ug/ml). Upon 12 hours caspase 3/7 or western blotting assay was performed as described above.

Soft agar colony formation assay.

D283-MED and ONS-76 cells were transfected with miR34a expressing vector or empty control vector. Following 24 hours 10.000 cells were plated in the appropriate medium in 0.35% agar over a 0.5% agar base. Three plates were plated for each transfection (miR34a and empty vector) or untrasfected cells. Medium was replaced every week. Following eight weeks colonies were counted.

Patient tumor source.

Control human tissues were obtained from the NICHD Brain and Tissue Bank for Developmental Disorders, at the University of Maryland, Baltimore, Maryland, USA (see Table 3).

Surgical MB specimens were from the Department of Neurosurgery, Santobono/Pausillipon Hospital, Naples, Italy. All of the specimens were obtained at the time of diagnosis, prior to radiation therapy or chemotherapy, and they were subjected to histopathological review according to the WHO criteria (see Table 4).

RNA was extracted from tissue samples as described above. Syber green Real Time PCR was performed as described above. The two-tailed Mann-Whitney test was used for p-values calculations.

| Sample | Geneder | Origins | Age of Death | | Cause of Death | DDctmiR34a | DDctmiR34b | DDctmiR34c |
			years	days				
C1	M	African American	0	5	Congenital Heart Defect	0.0003485	0.005645265	0.007459893
C2	M	Caucasian	0	96	Bronchopneumonia	0.0001471	0.000546491	0.000624322
C3	M	African American	1	123	Dehydration	0.0006622	0.00082695	0.000911772
C4	M	Caucasian	0	119	Bronchopneumonia, Acute	0.0014122	0.00063039	0.000829206
C5	F	Caucasian	0	20	Pneumonia	0.0005040	0.000816189	0.000984741
C6	M	Caucasian	4	258	Drowing	0.0077462	0.005678301	0.006293369
C7	M	African American	0	68	Asphyxia	0.0032145	0.003607516	0.004983445
C8	F	African American	0	62	Pneumonia	0.0011743	0.000618703	0.001002884

Table 3. Additional data of control samples. *List of control samples analysed by using real-time RT-PCR detection assay for evaluation of miR34a expression. The final column presents the means of the miR34a, miR34b and miR34c C-t values normalized for sn-U6 RNA C-t values*

.

patient	Gender	Age at diagnosis (months)	Follow-up (months)	Histology (OMS 2000)	M stage (Chang)	note	DDct miR34a	DDct miR34b	DDct miR34c
MB1	F	35	1	large cell	M3	dead from disease	0.000439562	0.000164754	0.00000092
MB2	F	89.75	34	classic	M0	alive	4.03733E-05	2.18233E-05	1.77896E-05
MB3	F	26	24	desmoplastic	M0	alive	0.000187749	4.7404E-05	0.0000026
MB4	F	123.75	6	classic	M0	alive	0.000150429	7.873E-05	5.12863E-05
MB5	F	64.25	18	classic	M0	dead from disease	1.90E-09	0.000232943	1.26785E-05
MB6	M	76.25	17	classic	M0	alive	1.02598E-05	0.000140319	7.31007E-06
MB7	M	68.5	36	desmoplastic	M2	alive	0.000132799	0.000576276	0.0000033
MB8	F	168.5	15	classic	M0	alive	4.94992E-05	5.61323E-05	1.1765E-05
MB9	M	127.5	10	anaplastic	M0	alive	0.000172207	9.55637E-05	0.0000061
MB10	M	29	4	classic	M0	alive	0.000814396	0.00142609	0.0000064

Table 4. Additional data of patient tumor samples. *List of the MB patients from whom the samples were surgically removed and then analyzed be using a real-time RT-PCR detection assay for the evaluation of miRNAs expression. The final column presents the means of the miR34a, miR34b and miR34c C-t values normalized for sn-U6 RNA C-t values.*

Adenovirus infections.

6-well plated 200.000 SH-Sy5y cells were infected with mock or miR34a-expressing adenoviruses at a final title of 200 MOI. 24h following infection the medium was replaced with virus-free medium. 72h upon infection cells were harvested and western blot was performed, as described above. Adenovirus particles were purchased by the ViraQuest, Inc. North Liberty, IA 52317.

RESULTS

By computational analyses we noticed that several miR34a predicted targets are key genes of the Notch and Shh signaling: DLL1 (Delta-like protein 1) and Jag1, and Notch1 and Notch2, two ligands and two receptors of the Notch pathway, respectively, and Gli1, a key effector of the Shh pathway (Table 5).

	miRanda	TargetScan	PicTar	PITA
DLL1	18.13	90	14.53	-13.98
JAG1	----	77	4.82	-12.78
NOTCH1	----	95	9.64	-14.37
NOTCH2	----	68	5.17	-9.93
GLI1	16.15	----	----	2.05
* MET	16.82	88	8.56	-8.16
* BCL2	----	86	1.34	-14.23

Table 5. Selected miR34a targets. m*iR34a targets were selected by examining the target definitions of the indicated miRNA databases. Each database relies on different algorithms of target prediction and uses different read-out scales. For example PITA algorithm shows ΔΔG energetic values of the predicted miRNA/mRNA binding. Therefore the more negative is the value, the stronger the binding of the miRNA to the given site is expected. More then one miR34a-binding site is predicted for the DLL1, Notch1 and Jag1 3'UTRs (see also Fig. 8). In those cases the numbers given in Table 5 represent the score of the binding site with the best match for miR34a binding. If a database does not predict a selected gene as a miR34a target, the correspondent field is marked with the symbol "----". *= MET and BCL2 genes were chosen from among the experimentally validated miR34a targets as references for the scores values (Bommer et al., 2007; He et al., 2007).*

Given the crucial roles of these pathways in the MB context, we investigated whether miR34a could really target the selected genes and whether the miR34a expression has functional consequences in MB cells.

To evaluate whether miR34a effectively recognizes the 3'UTR of the selected genes in MB cells, we cloned the 3'-UTR full-length sequences downstream of a luciferase open reading frame (ORF) and the miR34a precursor sequence into a pCDNA3 vector.

As shown in Figure 8, transfection of miR34a expressing vector significantly down-regulated DLL1 reporter activity in Daoy cells, whereas no significant inhibition was observed on the Jag1, Gli1, Notch1 and Notch2 reporters. Moreover, mutations of the three miR34a binding sites within the DLL1 3'UTR completely abrogated the inhibitory effect of miR34a (Fig.9). These results indicated that miR34a directly targets DLL1-3'UTR in MB cells, by recognizing the predicted binding sites.
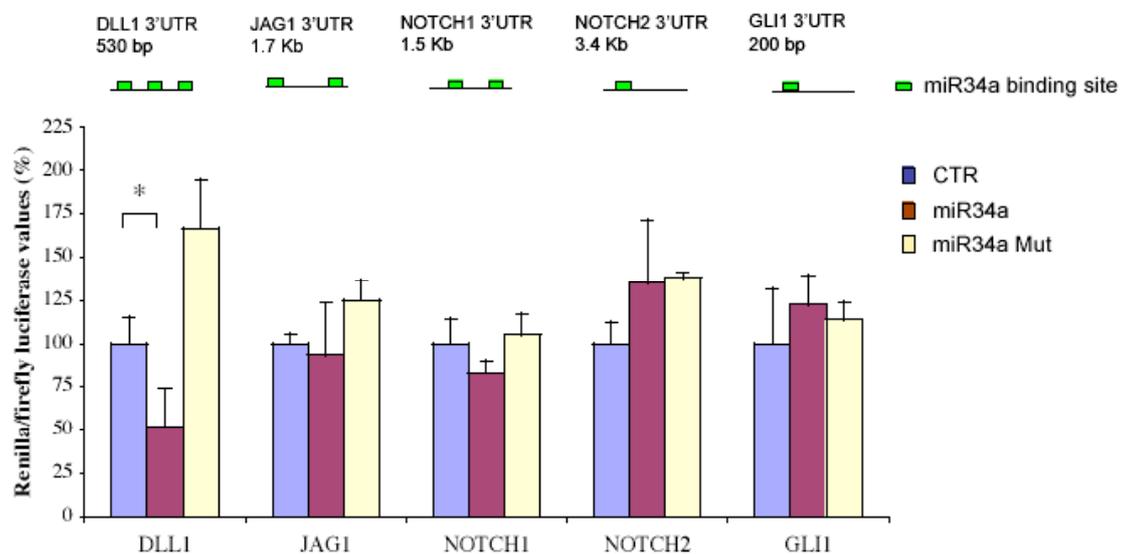

Figure 8. Direct recognition and validation of miR34a target genes using luciferase assays. *Daoy cells were co-transfected with 3'UTR reporter constructs, pGL3 control vector and empty vector, miR34a or seed-mutated miR34a. Representative 3'UTR pictures above columns show the number of miR34a binding sites predicted in each 3'UTR. Experiments were carried out in triplicate and the means are shown as percentages relative to the empty vector. Two-tailed upaired t-test was used for statistical analyses and p-values were calculated comparing the luciferase values of the empty vector- and the miR34a-transfected sample. Luciferase assays were performed following 24h from transfection.*
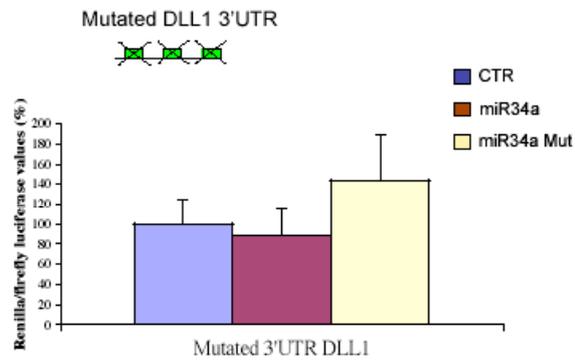
Figure 9. Luciferase assay of mutated DLL1 3-UTR reporter vector.
Daoy cells were cotransfected with mutated DLL1-3'UTR construct, pGL3 control vector and empty vector, miR34a or seed-mutated miR34a. Experiments were carried out in triplicate and the means are shown as percentages relative to the empty vector. Luciferase assays were performed following 24h from transfection. The mutated reporter construct was generated as described in material and methods.

We subsequently investigated whether miR34a can affect the endogenous expression of DLL1. Furthermore, since DLL1 is a known ligand of Notch1 and Notch2 receptors (Shimizu et al., 2000a; Shimizu et al., 2000b), we evaluated the possibility that miR34a expression can influence both pathways.

In-vitro studies have shown that miRNAs can induce translational inhibition in a time frame of even less than 1 h (Mathonnet et al., 2007), and *in vivo* studies, in cells, have indicated a down-regulation of target genes from 8 h following miRNA transfection (Wang, 2006). Therefore, we investigated time courses in Daoy cells starting from 6 h from miR34a transfection, while also transfecting duplicates at each time point for protein and RNA analyses.

As shown in Figure 10, miR34a expression, evaluated at each time point (see Figure 11), resulted in a transient reduction in DLL1 protein levels by 8 h, and then at 18 h from transfection. At these time points no decrease in DLL1 mRNA levels was detected (Fig.12), suggesting potential effect of miR34a on DLL1

45

translation. On the other hand, the recovery of DLL1 protein levels at the 12 h time point was supported by a transitory increase in its mRNA levels (Fig.12), which could be due to inherent feedback mechanisms of the Notch pathway, as previously described by Dr Shimojo and colleagues (Shimojo et al., 2008).
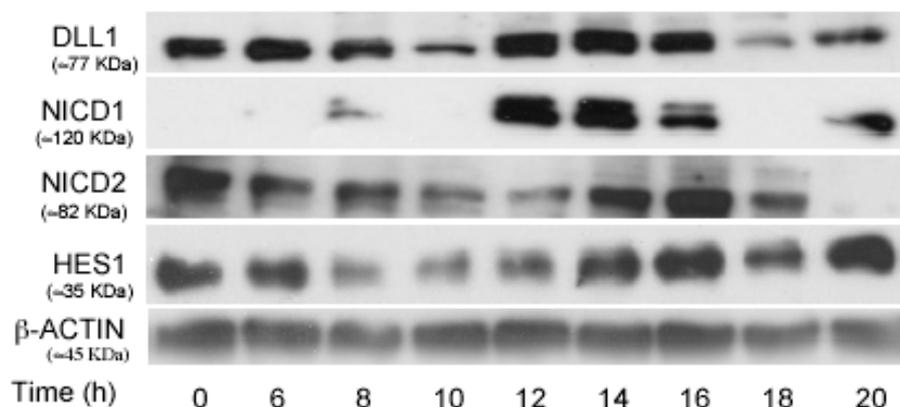

Figure 10. Time courses of miR34a over-expression in MB Daoy cells.
Western blotting of transient expression of miR34a in Daoy cells at different times post-transfection, using an antibodies panel for detection of the endogenous proteins: DLL1, Nicd1, Nicd2 and Hes1. The procedure used was as described in materials and methods.
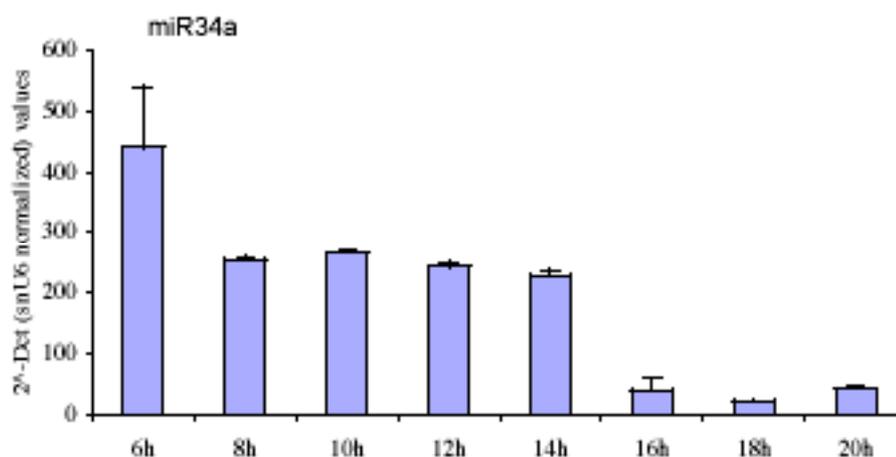
Figure 11. miR34a ectopic expression by real-time RT-PCR detection.
miR34a expression analysis, by real-time PCR assay, reveals miR34a over-expression at each time point from 6 h after transfection of Daoy cells. miR34a values were normalized according to sn-U6 RNA expression levels, and fold of expression compared to miR34a endogenous expression in Daoy cells are shown.
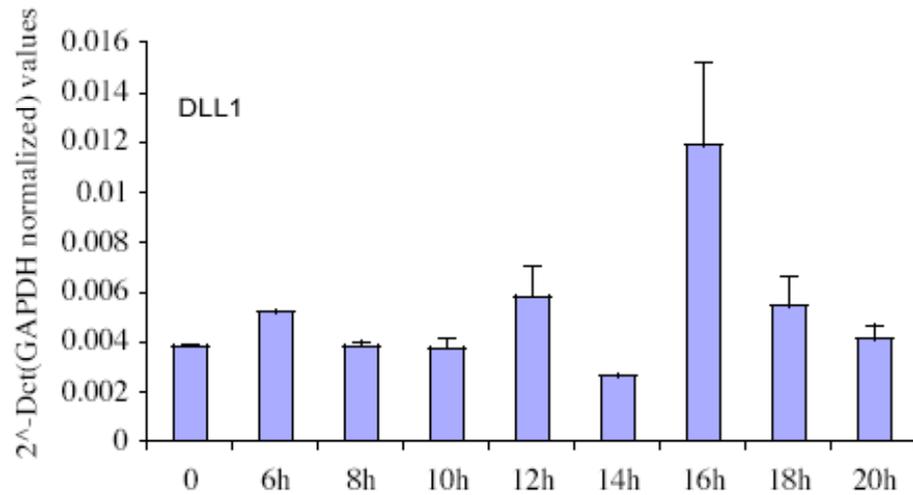
Figure 12. DLL1 expression analysis, upon transfection of miR34a, by real-time RT-PCR detection. *Real-time PCR analysis of DLL1 mRNA expression was performed from RNAs extracted by Daoy cells, at the indicated time points upon miR34a transfection. DLL1 values were normalized according to GAPDH expression. Experiments were performed in duplicates and averages of $2^{\wedge -Dct}$ values are shown.*

The down-regulation of DLL1 was followed by rapid Notch1 activation, as determined by Notch1 intracellular domain (NICD1) protein detection (Fig.10). The activation of downstream signaling was also confirmed by the expression induction of the CSL transcription factor-reporter construct, detected at 14 h from miR34a transfection of Daoy cells (Fig.13).
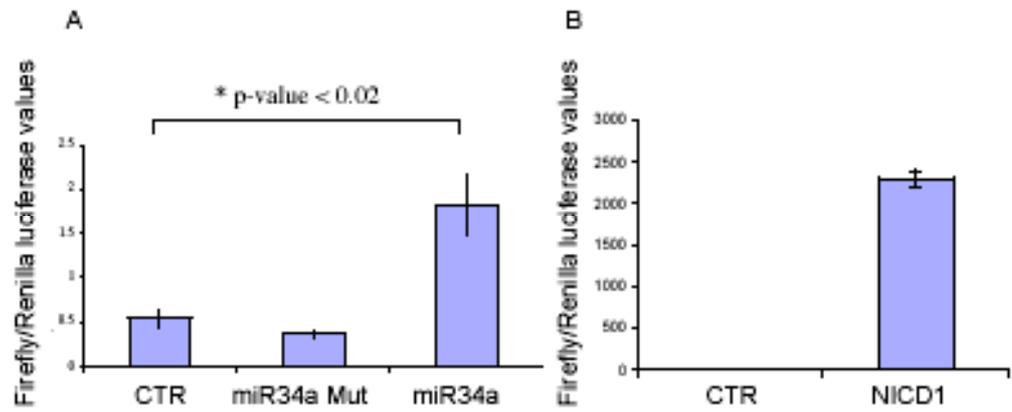
Figure 13. CSL transcription factor reporter assay by using protein lysates of miR34a transfected Daoy cells. A. *Daoy cells were co-transfected with CSL luciferase reporter construct, pRL-CMV vector and empty vector, mutated miR34a, wild type miR34a. (**B**) We transfected a NICD1 expressing vector as positive control for CSL reporter construct. Luciferase assays were performed following 14 hours from transfection, firefly luciferase values were normalized with renilla luciferase values, and averages of triplicates are shown. Two-tailed unpaired t-test was used for statistical analyses.*

The miR34a over-expression also resulted in a transient inhibition of Notch2 signaling, as seen by NICD2 and Hes1 protein down-regulation (Fig.10). A reduction in Hes1 mRNA confirmed the inhibition of the upstream pathway (Fig.14).
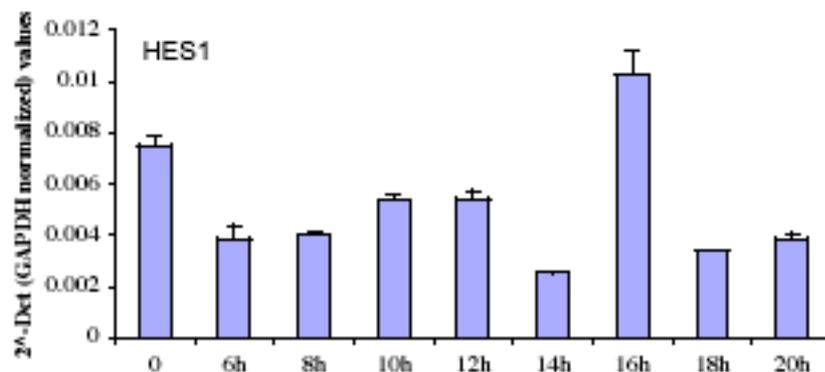
Figure 14. Hes1 endogenous expression analysis by real time RT-PCR detection, of Daoy cells after transfection of miR34a expressing vector. *Real-time PCR analysis was performed, by using Hes1specific primers, upon miR34a transfection in Daoy cells. Hes1 values were normalized according to GAPDH mRNA expression.*

Notch1 activation and Notch2 inhibition are not likely to be results of gene expression variations, since the mRNA levels did not follow the same trends in endogenous expression (Fig.15A and Fig.15B).
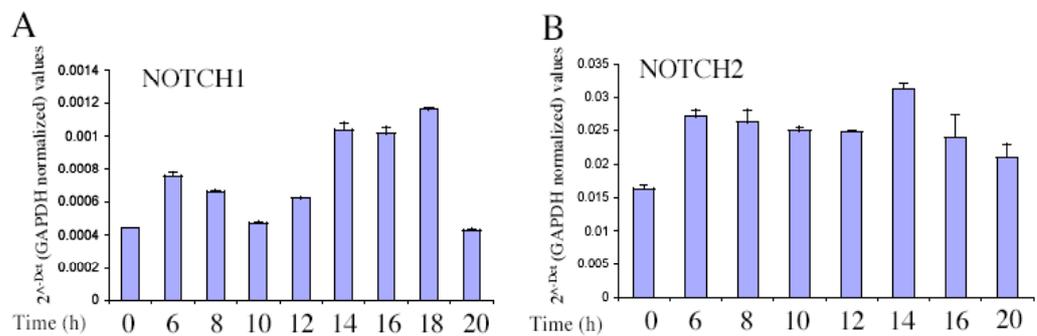

Figure 15. Notch1 and Notch2 endogenous expression upon miR34a transfection. *A. Real-time PCR analysis was performed, by using Notch1 or Notch2 (B) specific primers, upon miR34a transfection in Daoy cells. Notch1 and Notch2 values were normalized according to GAPDH mRNA levels of expression.*

Consistently with luciferase assays results reported in figure 8, transfection of the seed mutated miR34a, as negative control experiment, did not have any effects on DLL1 protein levels (see Fig.16).
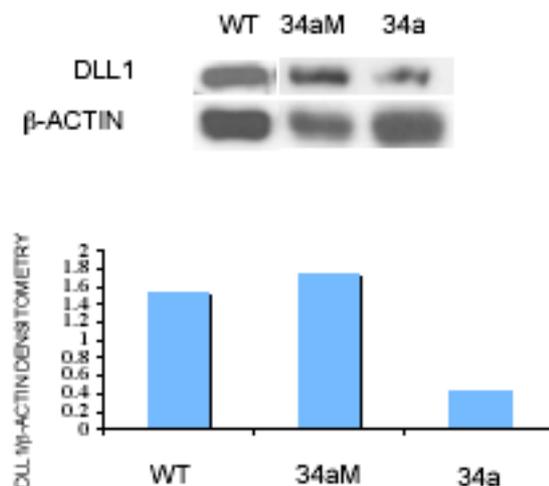
Figure 16. Western blot analyses of miR34a or seed mutated miR34a transfected Daoy cells. *Western blot of Daoy cells at 18 h from transfection of miR34a or seed-mutated-miR34a using an anti-DLL1 antibody. Non-transfected Daoy cells were used as control. The densitometric quantification of DLL1 band normalized with β-actin expression is shown below.*

Time courses were also performed in an other MB cell line (D283-MED), which showed similar results (Fig.17). In this case, we saw DLL1 protein down-regulation at 10 h post-transfection, followed by strong Notch1 activation. At the same time, Notch2 signaling was inhibited and the Hes1 protein was found down-regulated.
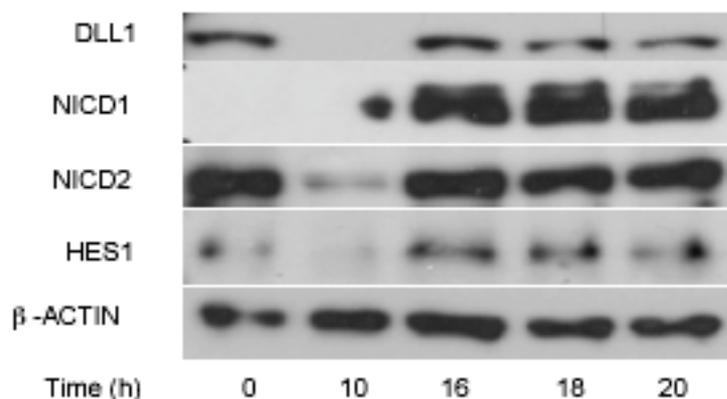

Figure 17. Time courses of miR34a over-expression in MB D283-MED cells. *Western blotting of miR34a-transiently transfected D283-MED cells at different times post-transfection, using an antibodies panel for detection of the endogenous proteins: DLL1, Nicd1, Nicd2 and Hes1. The procedure used was described in materials and methods.*

These results indicate that ectopic expression of miR34a in MB cells transiently down-regulates DLL1 protein levels and also influences the Notch1 and Notch2 pathways.

Previous studies have demonstrated that the soluble dominant-negative form of DLL1 inhibits cell proliferation in Daoy and D283-MED cells (Hallahan et al., 2004), and we also observed inhibition of proliferation of Daoy cells upon transfection of DLL1-Sh RNA constructs (Fig.18 and Fig.19). Moreover the Notch1 and Notch2 pathways have shown opposite effects in MB cells: Notch1

activity inhibited cell growth, whereas Notch2 signaling and Hes1 expression supported cell proliferation (as already shown by Fan et al., 2004).

Altoghether, these findings suggested that miR34a expression has an anti-proliferative effect in MB cells.
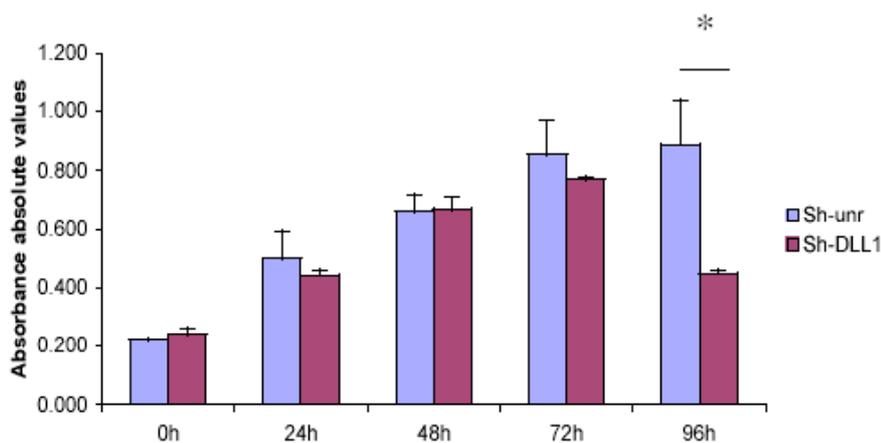

Figure 18. MTS proliferation assay of Daoy cells upon transfection of DLL1 sh-RNAs. *MTS proliferation assay was performed in Daoy cells at indicated time points upon transfection of a pool of three different sh-RNA constructs tareting the DLL1 sequence. Significant impairment of proliferation was detected at 96h from transfection (* = p-value < 0.04).*
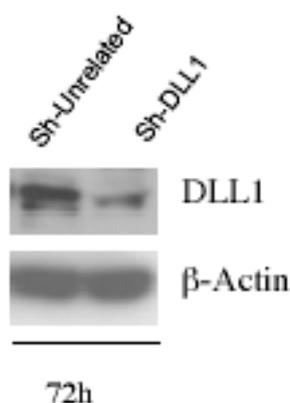

Figure 19. Expression levels of DLL1 protein upon DLL1-sh-RNA transfection in Daoy cells. *Western blot analysis was performed in Daoy cells 72h from transfection of a pool of 3 different sh-RNAs expressing vectors targeting the DLL1 sequence, or an unrelated- sh RNA by using anti-DLL1 and β-actin antibodies.*

51

To investigate the functional effects of miR34a in MB cells, we generated miR34a stable clones in Daoy cells (Fig.20).
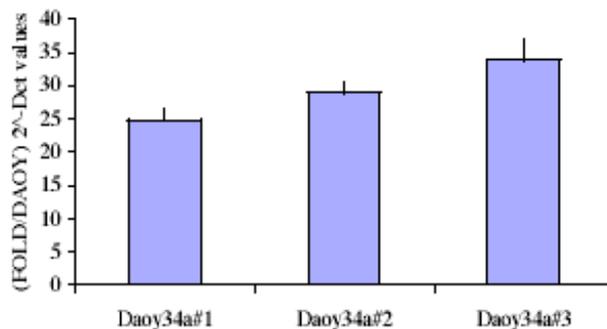

Figure 20. miR34a expression by real-time RT-PCR detection in Daoy stable clones. *miR34a expression in three different stable clones is shown as fold of expression compared to endogenous miRNA expression in Daoy cells. sn-U6 RNA was used to normalize themiR34a expression values.*

These clones showed a reduction in the DLL1 protein and down-regulation of NICD2 intracellular levels and Hes1 expression (Fig.21). Of note, activation of Notch1 was observed only in two out of three clones. We postulate that given the role of Notch1 in MB cells, survival mechanisms might have been selected to inhibit Notch1 activation in those cells (see western blot analysis of clone#3).
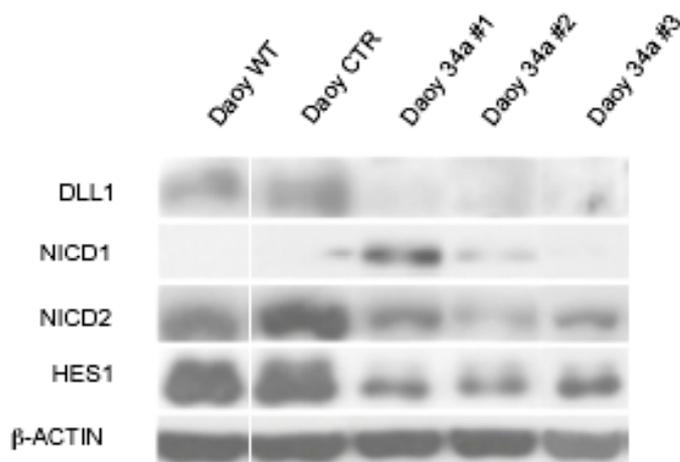

Figure 21. Western blot analyses of Daoy stable clones. *Stable miR34a clones (clones 1, 2 and 3), one stable empty vector clone and unselected Daoy cells were subjected to Western blotting using the indicated antibodies panel.*

Nevertheless, the MTS cell proliferation assay and FACS analysis for Annexin V detection revealed significant impairment of proliferation and a higher fraction of apoptotic cells in all the miR34a-overexpressing clones, as compared to the empty vector control clone (Fig.22 and Fig.23). These results were in agreement with behavior of stable clones in culture, which grew slower than control clones and wt cells, and then spontaneously died.
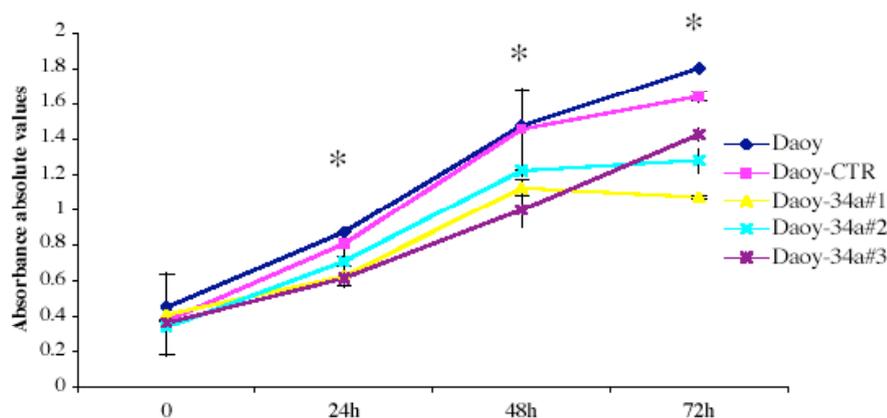

Figure 22. MTS proliferation assay of Daoy clones over-expressing miR34a. *MTS proliferation assay performed on stable clones and Daoy cells, as described in materials and methods. The absorbance means were evaluated from triplicates under normal serum conditions. *= p-value <0.02 (calculated for absorbance values of each clone compared with the control clone).*
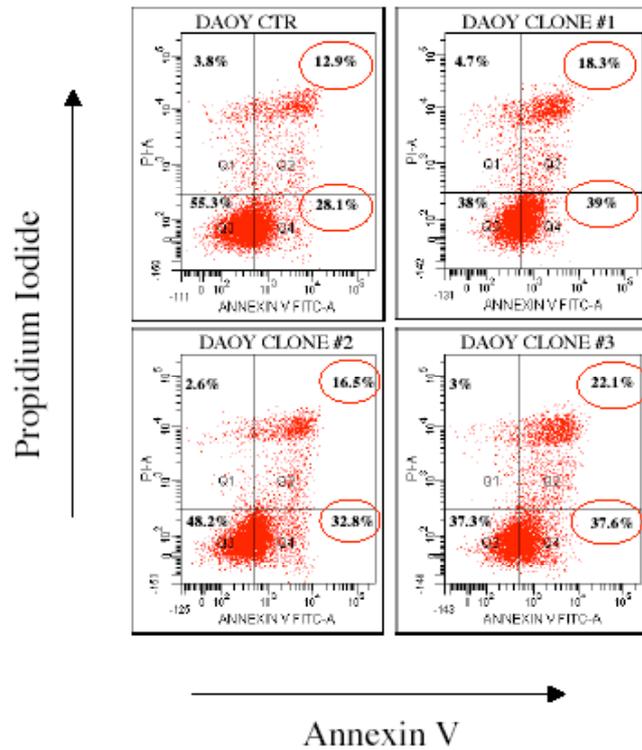
Figure 23. Apoptosis detection by FACS analyses of miR34a over-expressing stable clones. *Basal apoptosis of stable clones grown under the same selection conditions was investigated by FACS assay. Percentages of cells in early and late apoptosis (Q4 and Q2 squares, respectively) are marked with red circles.*

The miR34a stable clones also showed a more differentiated phenotype (see Fig.24), therefore we investigated whether miR34a over-expression was influencing the cellular differentiation rate.
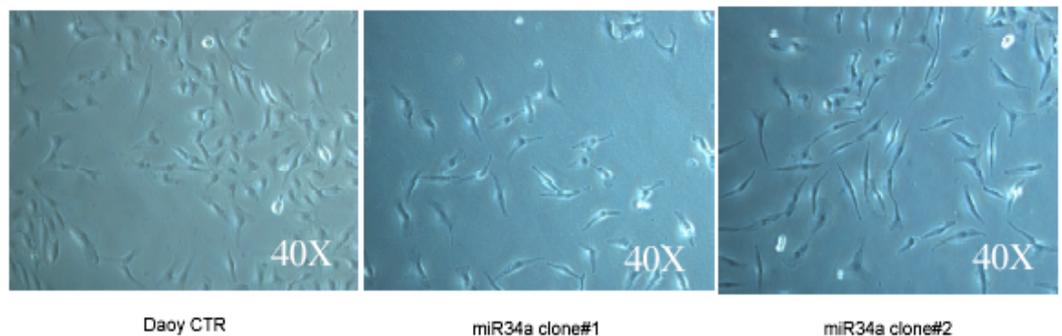

Figure 24. Morpfological features of miR34a stable clones resemble a more differentiated phenotype. *Morphological phenotype analysis of the miR34a stable clone#1 and clone #2, compared to a stable clone containing the control vector, under light microscope (Leika DMIL, 40X 0.22 magnification), showing extensive neurite out-growth processes and resembling a more differentiated phenotype.*

As shown in figure 25, we analyzed a panel of expression of differentiation markers, detecting high levels of the glial marker GFAP (Fig.25). Of note, Daoy cells have been previously reported to specifically express glial-specific protein under different conditions, such as induction of differentiation by phenylbutyrate treatment or epidermal growth factor (EGF) stimulation (Li et al 2004, Shen et al 2001).
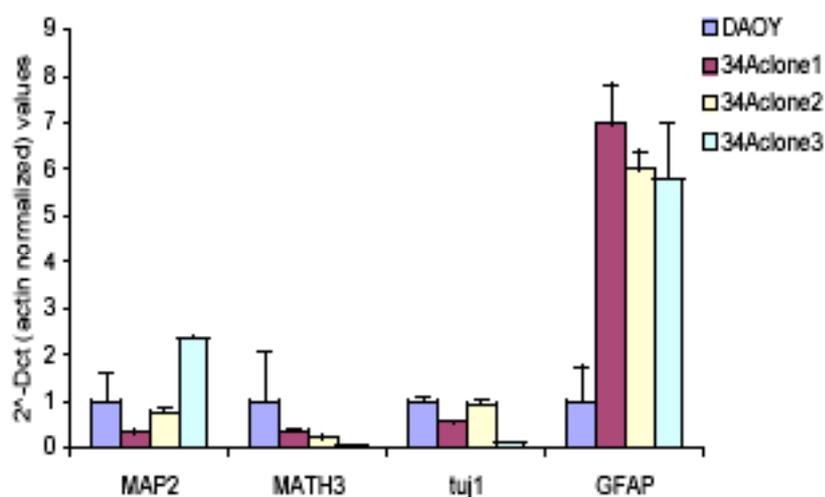

Figure 25. Expression analyses of differentiation markers by real time PCR assay of miR34a Daoy stable clones. *Real-time PCR detection of differentiation markers reveals induction of a glial phenotype, as shown by up-regulation of GFAP mRNA expression. Experiments were performed in duplcate, and average of β-actin normalized expression values are shown.*

In agreement with the phenotype observed in the Daoy stable clones, transient transfection of miR34a resulted in inhibition of proliferation and induction of apoptosis in MB ONS-76 and D283-MED cells (Fig.26 and Fig.27). Interestingly, co-transfection of DLL1 expressing vector rescued the caspase3/7 activation induced by miR34a expression in Daoy cells (Fig.28 and Fig.29).
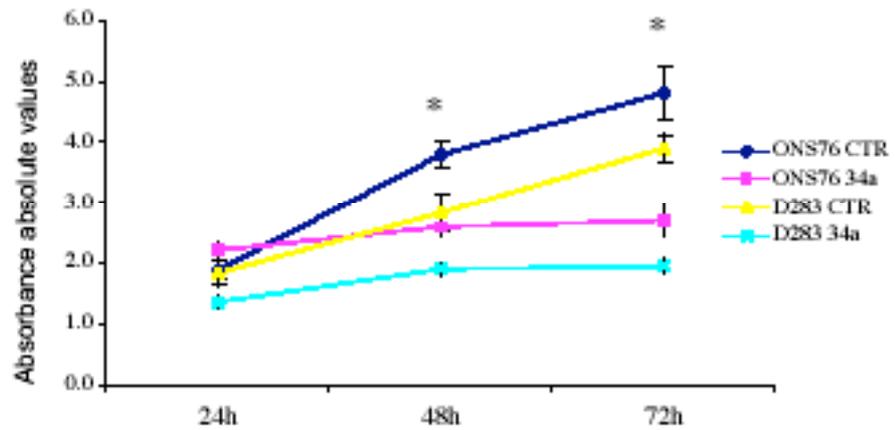
Figure 26. MTS proliferation assay of MB ONS76 and D283-MED cells upon transfection of miR34a expressing vector. *MTS proliferation assay performed on miR34a or empty vector transiently transfected ONS76 and D283-MED cells. The absorbance means were evaluated from triplicates under normal serum conditions. Folds of the means at each time point calculated with the time 0 h are shown. * = p-values were calculated as <0.02 for ONS76 at 48h and 72h time points and D283-MED at 72 h time point.*
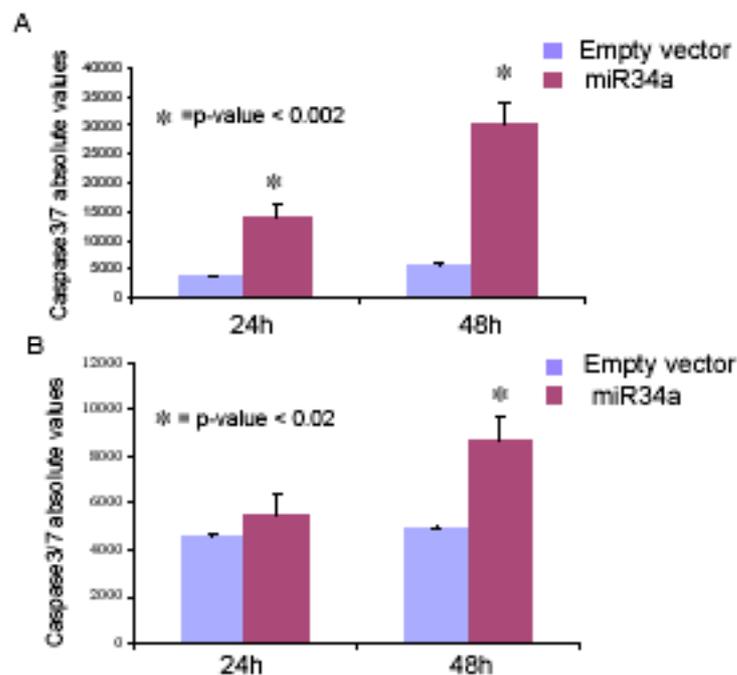

Figure 27. Caspase3/7 assay in ONS76 and D283-MED cells upon miR34a expression. A. *Caspase-3/7 assays were carried out in ONS-76 and D283-MED (B) at 24 h and 48 h after transfection of miR34a or an empty control vector, as described in materials and methods. p-values were calculated comparing the caspase 3/7 activity values of the miR34a transfected samples with empty vector transfected samples, by using two-tailed unpaired t-test analyses.*
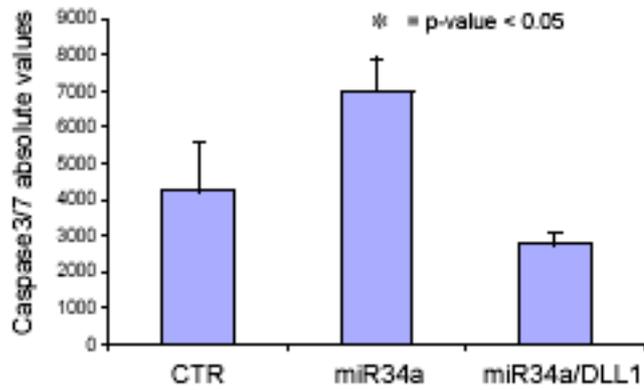
Figure 28. Caspase 3/7 activity upon transfection of miR34a or miR34a and DLL1. *Caspase 3/7 assay was performed 24 hours from co-trasfection of miR34a and murine DLL1 expressing vector or miR34a and empty vector. Average and standard deviations of the results of triplicates are shown.*
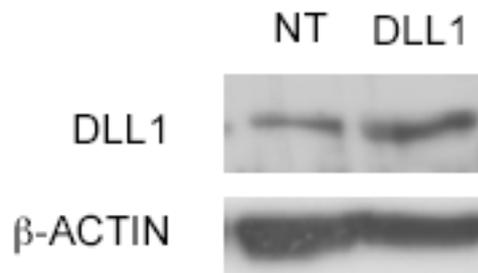

Figure 29. Western blot analysis of Daoy cells upon transfection of murine DLL1 expressing vector. *Western blot analysis was performed 24 hours from transfection of murine DLL1 expressing vector or empty vector in Daoy cells, by using DLL1 and β-actin specific antibodies.*

Moreover, *in-vitro* assays of tumorigenicity also showed a significant reduction in soft agar colony formation, upon miR34a over-expression, in both ONS76 and D283-MED cells (Fig. 30).
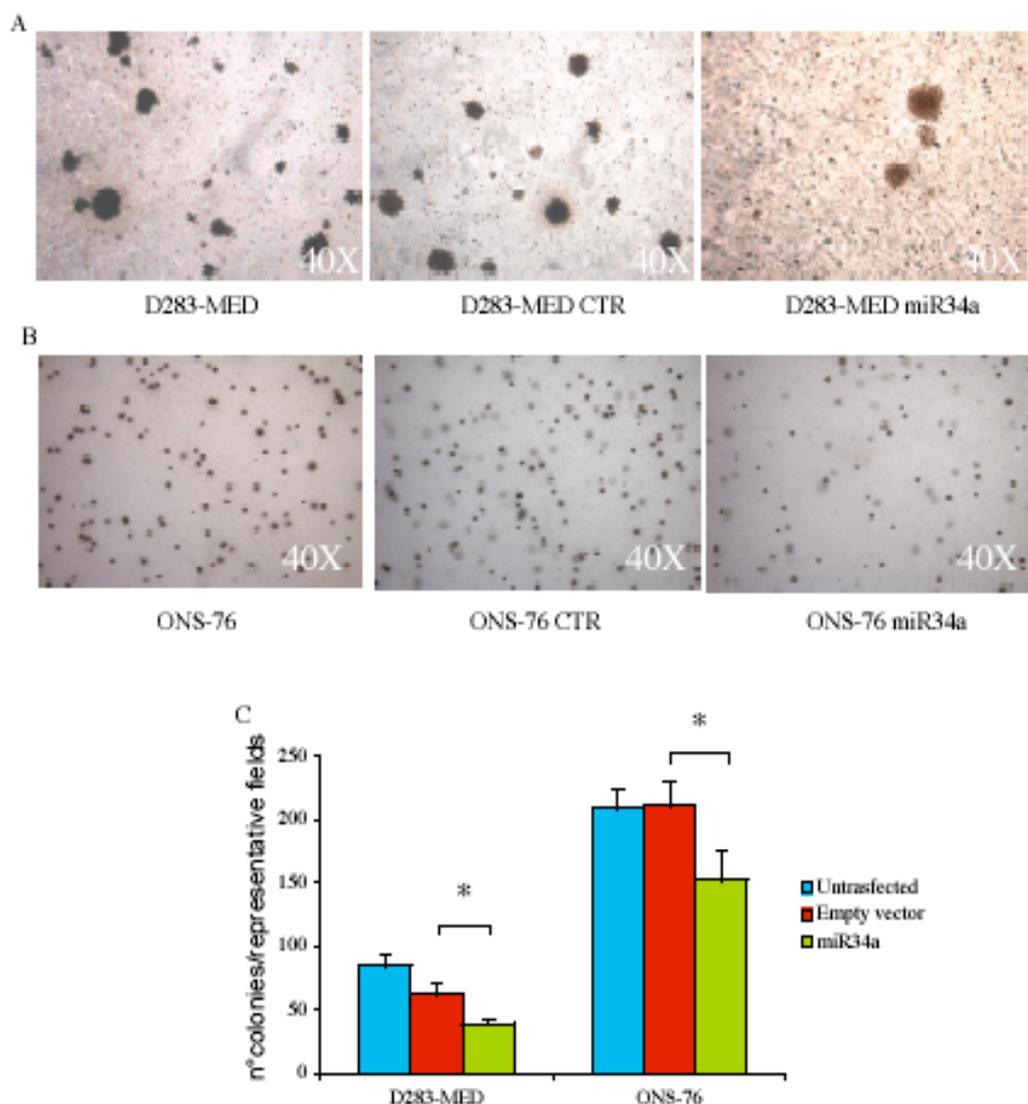
Figure 30. miR34a expression impairs soft agar colony formation of D283-MED and ONS76 cells. *A. and B. Representative fields of soft agar colony formation at 8 weeks upon transfection of empty vector or miR34a expressing vector or untrasfetced D283-MED and ONS-76 cells. C. Colony number average was calculated from three representative fields of each plate. Three plates for each sample (untrasfected and empty vector or miR34a transfected) were counted (*= p-value < 0.001).*

Altogether, these results indicate that miR34a can impair cell proliferation and *in-vitro* tumor growth and induce differentiation processes and apoptosis in MB cells. Furthermore, DLL1 downregulation can contribute to the apoptotic effect observed in Daoy cells.

In order to evaluate a possible involvement of miR34a in MB tumorigenesis, we investigated whether it was deregulated in human MB tumors. We also analysed the expression of the other miR34 family members, miR34b and miR34c, which share high sequence homology with miR34a. Interestingly, all of the miR34 family members were down-regulated in ten MB tumors and three MB cell lines, compared with eight non-tumoral human cerebellum samples (Fig.31).
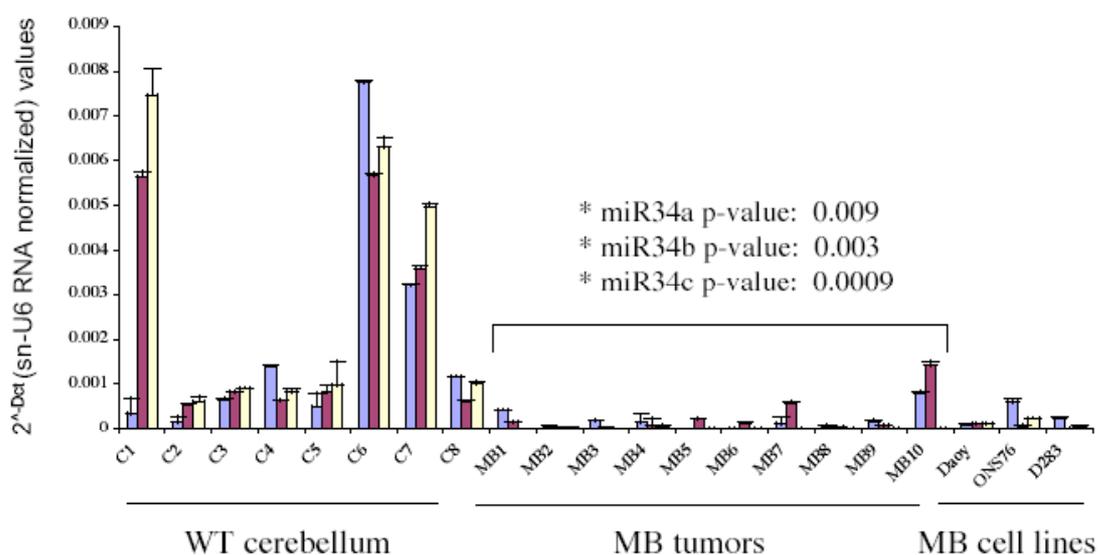

Figure 31. **miR34s expression analyses in human MB tumors.** *mir34a, miR34b and miR34c expression analysis by real-time PCR in human MB tumors, three different MB cell lines and human normal cerebellum samples. p-values were calculated by using two-tailed Mann-Whitney test. (for patients follow up and human normal cerebellum features see also Table 3 and 4 in material and methods).*

To investigate functional effects of the endogenous miR34a in MB cells, we transfected a miR34a-2'-O-methyl antisense oligoribonucleotide (miR34a-2-O-Me) to specifically block endogenous miR34a functions, and stimulated Daoy cells with the genotoxic agent doxorubicin, a p53 and miR34a activator (as previously described by He et al., 2007). Real-time expression analyses of $p21^{waf1}$ mRNA levels (known target of p53 transcription factor) and miR34a endogenous levels, confirmed the activation of p53 in Daoy cells, upon doxorubicin stimulated (see Fig.32).
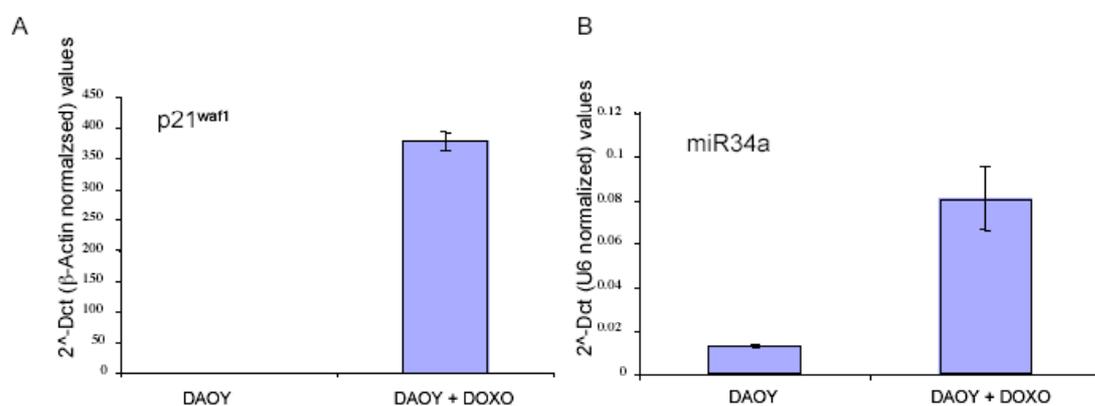
Figure 32. Expression analyses of p21^{waf1} and miR34a in doxorubicin stimulated Daoy cells. A. *Daoy cells were stimulated with 0.2ug/ml doxorubicin. Following 12 hours total RNA was extracted and real time PCR analyses was performed by using p21^{waf1} or miR34a (**B**) specific primers. Average of duplicates of p21^{waf1} and miR34a expression values are shown.*

We then compared the apoptotic effects of doxorubicin stimulation in non-transfected cells, and Daoy cells transfected with miR34a–2'-O-Me or an unrelated-2'-O-Me (un-2-O-Me). As shown in Figure 33, transfection of miR34a–2'-O-Me resulted in attenuation of caspase3/7 activity, thus suggesting that the endogenous miR34a is involved in the induction of p53-mediated apoptosis in Daoy cells.
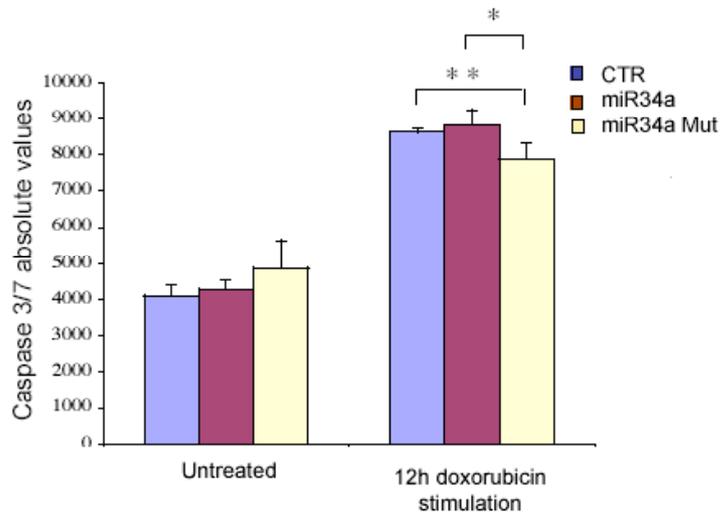
**Figure 33. Endogenous miR34a is involved in induction of apoptosis upon doxorubicin stimulation in Daoy cells.** *Caspase 3/7 assay upon 12 hours of doxorubicin stimulation, of non-transfected or previously transfected with unrelated or miR34a-2-O-methyl antisense oligos Daoy cells. *= p-value < 0.03; **= p-value 0.05.*

Interestingly, despite the increase in DLL1 mRNA levels (Fig. 34), doxorubicin stimulation resulted in DLL1 protein down-regulation (Fig. 35) and transfection of miR34a-2'-O-Me partially recovered the DLL1 protein levels (Fig.35). These results indicate that the endogenous miR34a can regulate the DLL1 protein expression.
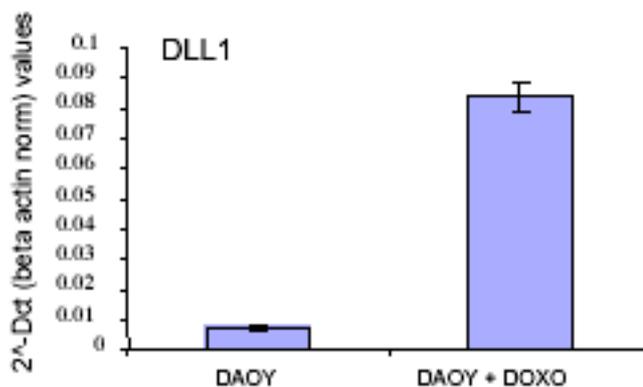

Figure 34. Real time PCR analysis of DLL1 gene expression upon doxorubicin stimulation. *Real time PCR expression analysis by using DLL1 specific primers reveals induction of expression upon 12 hours of doxorubicin stimulation. Average of duplicates experiments normalized with β-Actin expression values is shown.*
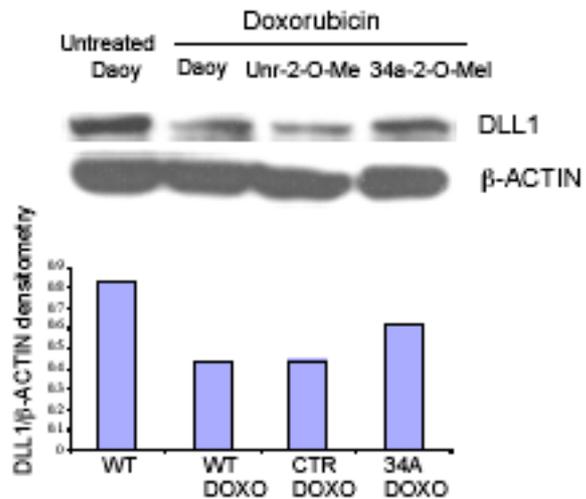
Figure 35. Transfection of miR34a-2'-O-Me partially rescues DLL1 protein levels upon doxorubicin stimulation. *Western blotting analysis was carried out by using anti-DLL1 antibodies, on untreated or doxorubicin stimulated Daoy cells, untrasfected or 2'-O-Me transfected cells, as indicated in the panel. The densitometric quantification of DLL1 band normalized with β-actin expression is shown below.*

Time course experiments of doxorubicin stimulated Daoy cells also revealed a transient down-regulation of DLL1 protein levels (Fig.36), despite the induction of the mRNA expression, which was observed at each time point (see Fig.37). This effect was not observed in miR34a-2'-O-Me transfected cells (Fig.36), therefore further confirming that the induction of the endogenous miR34a, upon p53 activation induces down-regulation of the direct target DLL1. Induction of both miR34a and *p21^{waf1}* mRNA levels were analysed at each time point, and results are shown in Fig.38.

Of note, doxorubicin stimulation also induced a down-regulation of NICD2 and a late and weak inhibition of Hes1, however no activation of Notch1 was observed (Fig.36). NICD2 inhibition was only weakly reverted by miR34a-2'-O-Me transfection suggesting that the down-regulation of its expression could be mediated by indirected mechanisms of action induced by doxorubicin treatment. As further proof, it was observed that p53 activation inhibits Notch processing by

transcriptionally inhibiting the expression of presenilin, a known component of the

γ-secretase complex (Laws & Osborne, 2004).
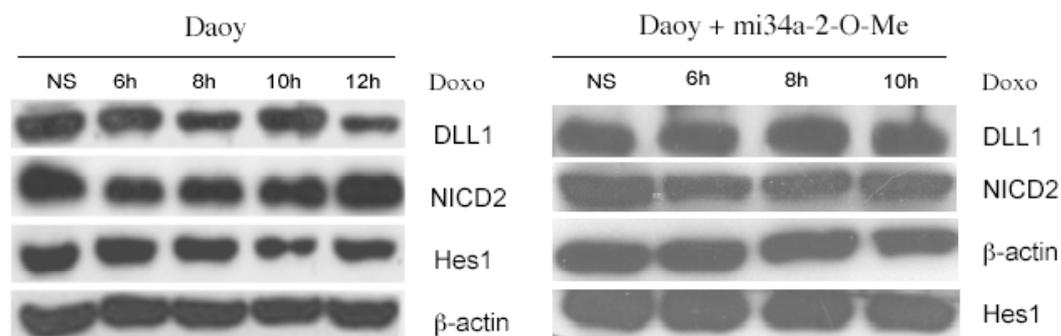
Figure 36. Time courses experiments of doxorubicin stimulated Daoy cells. *Western blot analysis of untrasfected or miR34a-2'-O-Me transfected (right panel) Daoy cells, not stimulated (NS) or stimulated with for doxorubicin for the indicated time. DLL1, NICD2, Hes1 and β-Actin protein expression was evaluated with specific antibodies.*
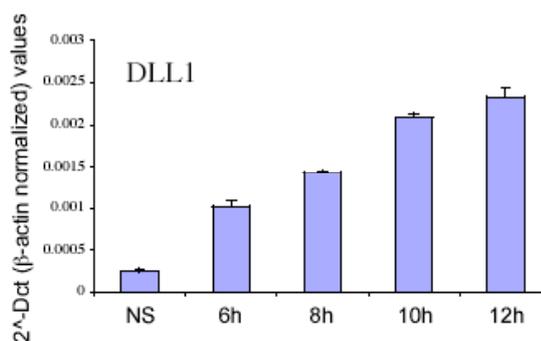
Figure 37. Real time PCR analysis of DLL1 gene expression upon doxorubicin stimulation. *Real time PCR expression analysis of doxorubicin stimulated Daoy cells, reveals induction of DLL1 expression at each time point. Averages of duplicates experiments normalized with β-Actin expression values are shown.*
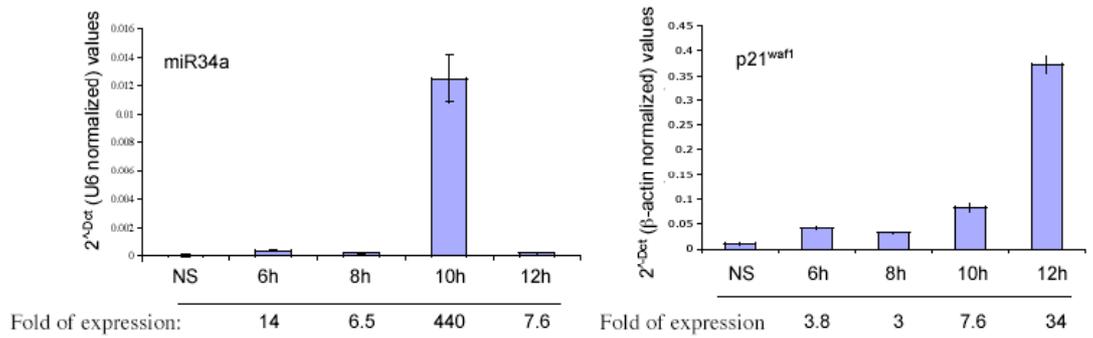
Figure 38. Real-time PCR analyses of endogenous miR34a and p21^waf1 expression in doxorubicin-stimulated Daoy cells. *Daoy, cells were treated with doxorubicin at a final concentration of 0.2ug/ml and RNA was extracted at indicated time points. Real time PCR analysis was performed by using miR34a and p21^waf1 specific primers. Average of duplicates experiments normalized with sn-U6 RNA and β-Actin relative expression values are shown. Fold of induction of miR34a and p21^waf1 shown below the charts represent the ratio with un-stimulated cells.*

Taken together these results indicate that endogenous levels of miR34a can regulate DLL1 protein expression in MB cells.

Thus, we subsequently investigated whether this process could be generalized in other cellular contexts. Since miR34a genomic region (chr1p36) is frequently deleted or rearranged in neuroblastoma tumors, which also show rearrangements within the miR34b/c genomic region (chr11q23) (Attiyeh et al., 2005), neuroblastoma cells could represent a useful tool to investigate the effects of the endogenous expression of miR34 family members on DLL1 protein levels. Therefore, we stimulated with doxorubicin the neuroblastoma SH-SY5Y cells, in which a reported deletion of chromosome 11q23 could affect miR34b/c expression (Kim et al., 2001), and the SK-N-BE and GIMEN cells, carrying deletion of chromosome 1p36, thus possibly affecting miR34a expression (Thiele CJ et al., 1998; Schleiermacher et al., 2003).

By luciferase assays we confirmed that miR34a expression down-regulates the DLL1-3'UTR reporter activity in the three neuroblastoma cell lines (Fig.39). Therefore the different cellular contexts do not inhibit the miR34a/DLL1-3'UTR binding, and miR34a can potentially down-regulate DLL1 in each cell line.
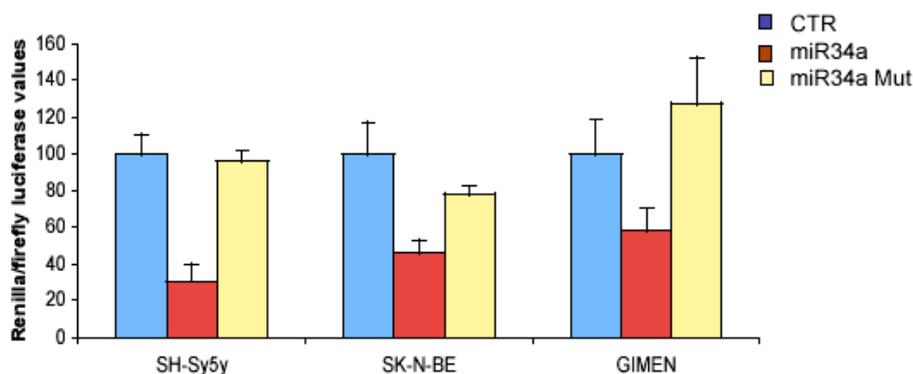
Fig.39. Luciferase assays of DLL1-3'UTR reporter vector in neuroblastoma cells. *SH-Sy5y, SK-N-BE and GIMEN cells were co-transfected with DLL1-3'UTR reporter vector, pGL3 control vector and empty vector, miR34a or seed-mutated miR34a. Experiments were carried out in triplicate and the means are shown as percentages relative to the empty vector. Luciferase assays were performed following 24h from transfection.*

We also stimulated MCF7 and MDA231 human breast cancer cells, in which wt and mutated p53 was reported, respectively (Gartel et al., 2003).

We stimulated Daoy cells as control and performed all treatments in duplicates, to allow real time mRNA expression analyses and western blot assays for protein levels detection.

As shown in Fig. 40, doxorubicin stimulation resulted in induction of miR34a in Daoy, SH-SY5Y and MCF7 cells, and induction of miR34b and miR34c in Daoy and SK-N-BE. At a lower rate, we also detected an induction of miR34b and miR34c expression in doxorubicin stimulated GIMEN cells, whereas MCF7 cells induced the expression of miR34a and miR34b, but not miR34c. As expected, the expression of any miR34 isoform was induced in treated MDA231 cells.

Interestingly, although DLL1 mRNA levels increased in all treated cells (Fig.42), western blot analyses revealed a strong correlation between miR34a expression and DLL1 protein downregulation (Fig.41).

Indeed, as shown in Fig.41, DLL1 protein levels were markedly down-regulated in Daoy, SH-SY5Y and MCF7 cells, whereas increased in GIMEN cells. No effect was observed in MDA231 cells.
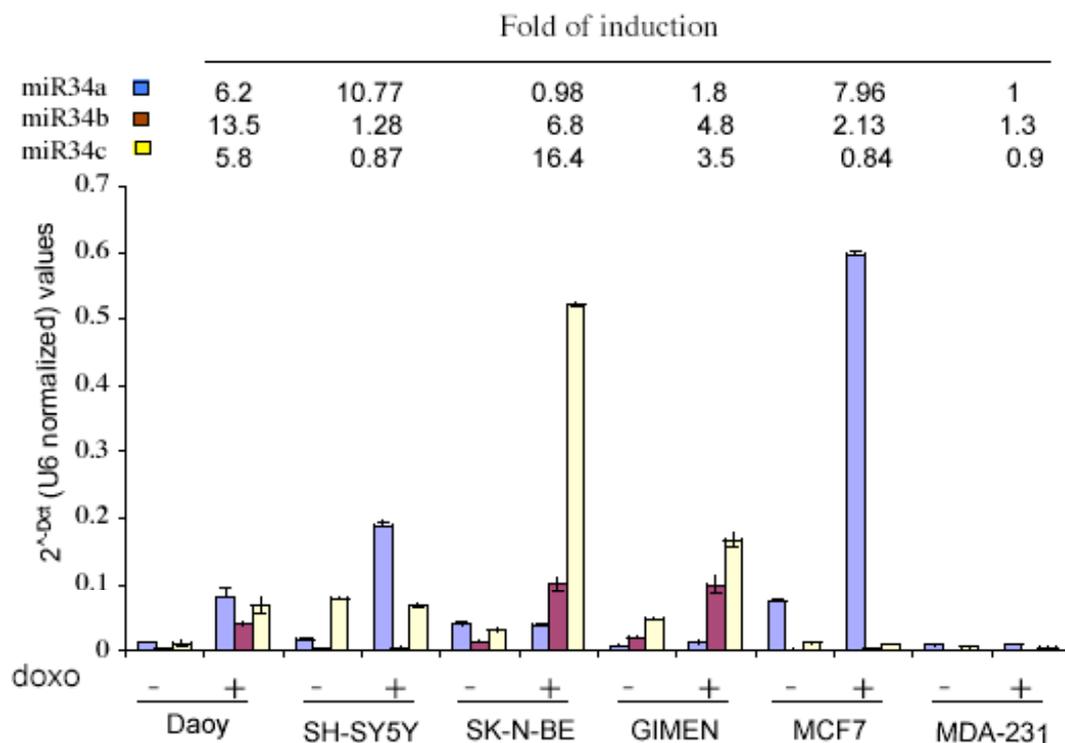
Figure 40. miR34a, miR34b and miR34c expression analyses in different cell lines upon doxorubicin stimulation. *miR34a, miR34b and miR34c expression analyses by RT-PCR of the indicated cell lines untreated or upon 24h of doxorubicin stimulation. Fold of expression shown above the graphic represent the ratio between treated and untreated cells, for each miRNA.*
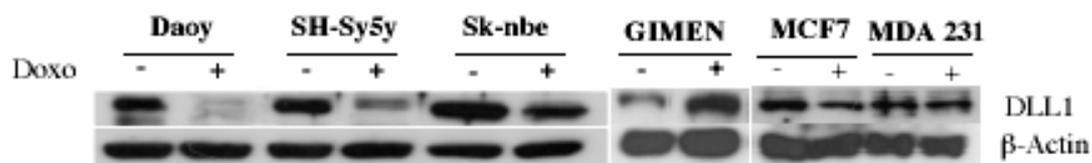
Figure 41. Western blot analyses of different cell lines upon doxorubicin stimulation. *Western blot analyses by using DLL1 and β-Actin specific antibodies, of doxorubicin stimulated or untreated cells.*
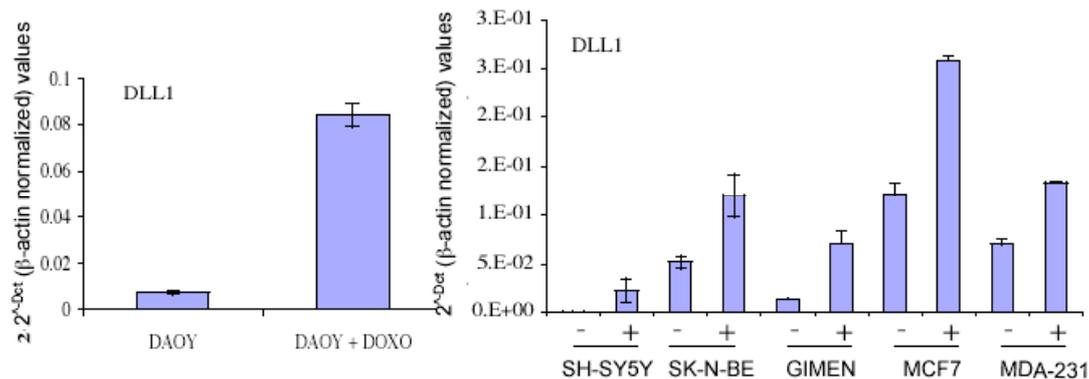
Figure 42. Real time PCR analysis of DLL1 gene expression upon doxorubicin stimulation of different cell lines. *Real time PCR analysis reveals induction of expression of DLL1 in the indicated tumor cell lines upon 24h of doxorubicin stimulation.*

Adenovirus infection may overcome the variability of cell transfection. Therefore to further validate the direct effect of miR34a expression on DLL1 protein levels, we infected SH-Sy5y cells with an adenovirus type 5 expressing the precursor miR34a or an empty virus clone. As shown in Fig.43, infection with miR34a expressing adenovirus markedly downregulated DLL1 protein levels.

Noteworthy, a weak but visible down-regulation of DLL1 protein levels was also observed in doxorubicin stimulated SK-N-BE cells (Fig.41), in which miR34a expression was not induced, but miR34b and miR34c reached the highest levels of induction among the treated cells (see Fig.40). Since the nucleotide sequences of miR34 isoforms are highly similar, we thus hypothesize that miR34b and miR34c might also target DLL1.

We cloned the miR34b/c cluster, as it maps within the genome: the two precursors miRNAs spaced by 400bp of genomic region, and co-transfected this construct with DLL1-3'UTR reporter vector in HEK293 cells. As shown in Fig.44 miR34b/c expression downregulated the DLL1-3'UTR reporter activity at the same rate of miR34a (Fig.44).

67
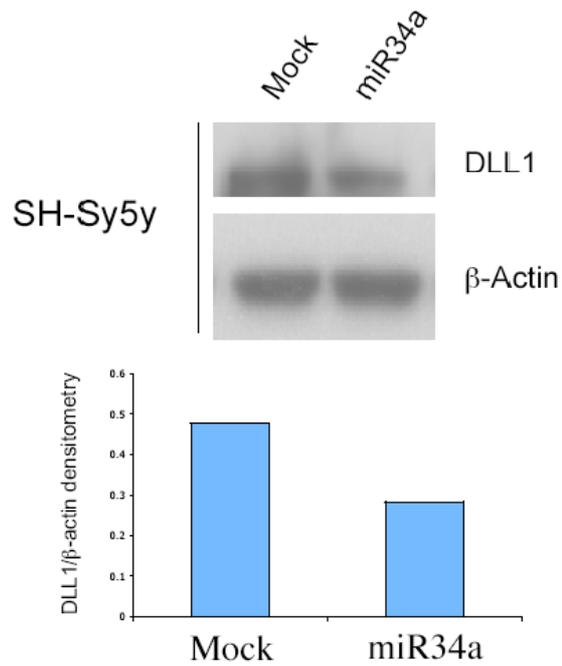
Figure 43. Western blot analysis of SH-Sy5y cells upon infection with miR34a expressing adenovirus. *Western blot analysis was performed in SH-SY5Y cells upon 48h from infection with miR34a expressing or mock adenoviruses. DLL1 and β-actin expression were detected by using specific antibodies. The densitometric quantification of DLL1 band normalized with β-actin expression is shown below.*
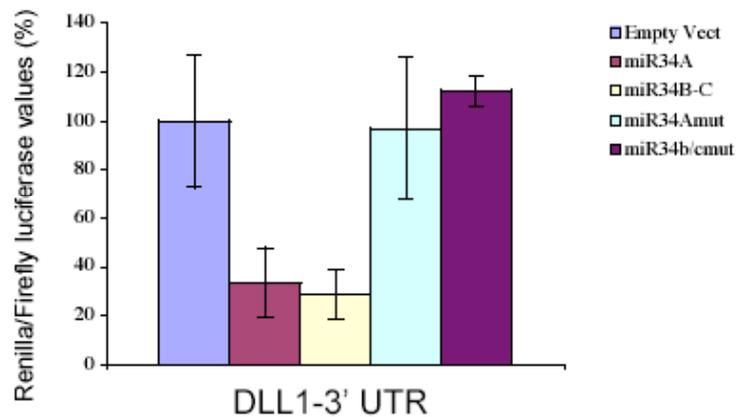
Figure 44. miR34b/c expressing vector down-regulates DLL1 3' UTR luciferase activity. *HEK293 cells were co-transfected with DLL1 3'UTR reporter construct, pGL3 control vector and empty vector, miR34a or seed-mutated miR34a, miR34b/c or seed-mutated miR34b/c. Experiments were carried out in triplicate and the means are shown as percentages relative to the empty vector. Luciferase assays were performed following 24h from transfection.*

68

Altogether these results indicate that the miR34a effects of DLL1 down-regulation observed in MB cells, can be generalized to other cellular context. Moreover, miR34a, miR34b and miR34c might sinergically act in mediating this effect.

DISCUSSION

By computational analyses we noticed that some miR34a predicted targets belong to the Notch and Shh pathway (Table 5, page 43), two signaling pathways required for survival and tumor growth of medulloblastoma cells (Berman et al 2002; Fan et al. 2006).

In this study, we investigated whether miR34a could effectively target these two pathways and have oncosuppressor activities in MB.

We report here that miR34a targets the Notch-ligand DLL1 by pairing its specific binding sites within the DLL1-3'UTR (Fig.8 and Fig.9). This effect translates into a transient down-regulation of DLL1 protein levels, observed upon either ectopic expression of miR34a (Fig.10; Fig.17; Fig.21) or induction of the endogenous miRNA (Fig.35; Fig.36). miR34a ectopic expression also resulted in inhibition of Notch2 signaling and activation of Notch1 receptor, an effect that we observed in Daoy and D283-MED MB cells (Fig.10; Fig.17; Fig.21).

DLL1 is known to bind Notch1 and Notch2 and activate each of these pathways in a non-autonomous manner (ligand and receptor expressed by two neighboring cells) (Ladi et al., 2005). However, the DLL1/Notch1 interaction within the same cell (a phenomenon known as cell-autonomous association) has also been shown to inhibit Notch1 signaling (Ladi et al., 2005; Sakamoto et al., 2002). We thus hypothesize that cell-autonomous association of DLL1/Notch1 would be a mechanism by which Notch1 signaling is maintained under inhibition in MB cells, given its inhibitory effects on cell proliferation (as already reported by Fan et al., 2004).

Indeed, in our time-course studies, down-regulation of the DLL1 protein was quickly followed by a massive NICD1 expression (see Fig.10 and Fig.17). Moreover, endogenous DLL1 re-expression is then followed by a marked inhibition

of Notch1 activation (see Fig.10). Such re-expression could result, at least in part, from Hes1 down-regulation, as it is known that Hes1 inhibits DLL1 expression (Shimojo et al., 2008). The reduction in the DLL1 protein levels also correlated with an inhibition of Notch2 signaling that we showed to occur at the same time as the reduction in DLL1 protein levels (see Fig.10; Fig.17), thus suggesting a role for DLL1 as an activator of Notch2 signaling. In agreement with this hypothesis the inhibition of either DLL1 or Notch2 impairs proliferation of MB cells (Hallahan et al. 04; Fan.X et al; Fig.18).

DLL1 protein down-regulation was also observed upon induction of the endogenous miR34a, via p53 activation, in Daoy cells; this effect was then reverted by miR34a-2'-O-Me oligo transfection (Fig.35; Fig.36). Moreover, in time course experiments, when the endogenous miR34a was induced, we detected a transient down-regulation of DLL1 (Fig.36), which is consistent with the results obtained upon ectopic expression of the miRNA (Fig.10).

It was previously shown that the miRNAs inhibitory effects on target genes, are sensitive to the relative concentrations of the target mRNA and miRNA (Mathonnet et al 2007).

We believe that the transitory effect on DLL1 down-regulation observed upon ectopic expression of miR34a could be referable, at least in part, to variations in DLL1 mRNA levels (Fig.10).

Indeed, an induction of DLL1 mRNA levels at the 12h time point (see Fig.12) correlated with the increase in DLL1 protein levels (Fig.10). A possible explanation could be that miR34a requires a time to inhibit translation of *de-novo* transcribed DLL1-mRNA; indeed at the 18h time point, DLL1 protein down-regulation happens again, in spite of its endogenous mRNA levels, which do not follow the same trend (se Fig.10 and Fig.12).

On the other hand, during doxorubicin stimulation of Daoy cells (Fig.36),

71

DLL1-mRNA levels increased at each time point (Fig.37). However, miR34a endogenous expression decreased between 6h and 8h time point (Fig.38). Therefore, in this case, we can hypothesize that the transient effect on DLL1 down-regulation could be referable to limiting concentrations of the endogenous miR34a.

Of note, in the time course of Fig.36, despite the down-regulation of DLL1 and the expression of the endogenous miR34a, we did not observe the Notch1 activation, and the down-regulation of NICD2 was observed very weakly reverted by trasfection of miR34a-2'-O-Me (Fig.36). These results appear to be in contrast with the previous data shown in figure 10, obtained upon ectopic expression of miR34a (Fig.10). However, they could be explained by the described crosstalk between p53 and Notch pathway, by which p53 inhibits the Notch processing by transcriptionally inhibiting presenilin1 expression, a known component of the γ-secretase complex (Laws & Osborne, 2004). This effect could explain the absence of Notch1 activation, in doxorubicin-stimulated cells, and the sustained inhibition of Notch2, even upon re-expression of DLL1 or transfection of the miR34a-2'-O-Me. Indeed, as shown in Figure 36, the inhibition of the Notch2 was clearly an early event, thus likely independent by the DLL1 down-regulation, which was then observed.

Taken together these results suggest a new mechanism by which p53 can interfere with the Notch pathway, down-regulating DLL1, via miR34a expression.

This mechanism seems not to be restricted to MB cells, since expression of endogenous miR34a, upon p53 activation, correlates with down-regulation of DLL1 in different tumor cell lines (Fig.40; Fig.41). Furthermore, a direct effect of DLL1 down-regulation upon miR34a ectopic expression was also validated in SH-Sy5y neuroblastoma cells (Fig.43).

Interestingly, we show that the expression of miR34b and miR34c can also impair DLL1-3'UTR reporter activity (Fig.44), suggesting that the three miR34

isoforms can sinergically regulate the DLL1 expression.

To evaluate functional effects of miR34a in MB cells, we generated miR34a-expressing Daoy stable clones, and also transiently over-expressed miR34a in different MB cell lines.

In these experiments miR34a was able to induce marked functional effects in MB cells. It impaired proliferation and soft agar colony formation, and induced apoptosis and differentiation processes (Fig.22-30). Moreover, depletion of miR34a also slightly impaired p53-induced apoptosis in Daoy cells (Fig.33).

These results suggest that miR34a can be involved in MB tumorigenesis and that its down-regulation could confer proliferative advantage to the tumor cells, contributing to the tumor behaviour.

Consistent with this hypothesis, we show that the expression of miR34a as well as miR34b and miR34c expression is lost in human MB tumors (Fig.31).

Since several miR34a targets, such as Bcl2 and E2F3 (Bommer et al., 2007; Welch et al., 2007), are also known regulators of apoptosis and cell proliferation, the functional effects mediated by miR34a are likely to be referable to the down-regulation of more than one target. However, reasonably, target recognition of miRNAs and their down-regulation efficacy, depend on the expression levels of both, miRNA and target, and can be cellular context-specific (Mathonnet et al 2007).

Here we show that endogenous levels of miR34a regulate DLL1 expression, and that the exogenous expression of DLL1 can revert the apoptotic effect mediated by miR34a, in Daoy cells (Fig. 28). These results suggest that DLL1 down-regulation can significantly support the functional effects mediated by miR34a in MB cells.

However, we can hypothesize that other targets will contribute in the induction and support of the biological effects mediated by miR34a in MB cells.

It is also noteworthy to note that one of the three miR34a-binding sites within the DLL1 3'UTR is highly conserved throughout the evolution. Since both the miR34a sequence and the p53 binding sites within the miR34a promoter region are also highly conserved in different species, it would be interesting to investigate whether the axis p53-miR34a-DLL1 is conserved in other species.

Indeed, the lack of p53, possibly correlated with lack of miR34a (which also shows the highest levels of expression in the cerebellar cortex (Dutta et al 2007), increases the incidence of MB from 15% to 95% in PTC heterozygous mice (Wetmore et al., 2001). Therefore, investigations of possible effects of the murine miR34a in MB mouse models, would also allow a deeper understanding of the roles of miR34a in the tumorigenesis of this cancer.

References:

Attiyeh, E.F., London, W.B., Mosse, Y.P., Wang, Q., Winter, C., Khazi, D., McGrady, P.W., Seeger, R.C., Look, A.T., Shimada, H., Brodeur, G.M., Cohn, S.L., Matthay, K.K. & Maris, J.M. (2005). *N Engl J Med*, **353,** 2243-53.

Bartel, D.P. (2004). *Cell*, **116,** 281-97.

Baskerville, S. & Bartel, D.P. (2005). *Rna*, **11,** 241-7.

Berman, D.M., Karhadkar, S.S., Hallahan, A.R., Pritchard, J.I., Eberhart, C.G., Watkins, D.N., Chen, J.K., Cooper, M.K., Taipale, J., Olson, J.M. & Beachy, P.A. (2002). *Science*, **297,** 1559-61.

Bernstein, E., Kim, S.Y., Carmell, M.A., Murchison, E.P., Alcorn, H., Li, M.Z., Mills, A.A., Elledge, S.J., Anderson, K.V. & Hannon, G.J. (2003). *Nat Genet*, **35,** 215-7.

Bommer, G.T., Gerin, I., Feng, Y., Kaczorowski, A.J., Kuick, R., Love, R.E., Zhai, Y., Giordano, T.J., Qin, Z.S., Moore, B.B., MacDougald, O.A., Cho, K.R. & Fearon, E.R. (2007). *Curr Biol*, **17,** 1298-307.

Borchert, G.M., Lanier, W. & Davidson, B.L. (2006). *Nat Struct Mol Biol*, **13,** 1097-101.

Bray, S.J. (2006). *Nat Rev Mol Cell Biol*, **7,** 678-89.

Brennecke, J., Stark, A., Russell, R.B. & Cohen, S.M. (2005). *PLoS Biol*, **3,** e85.

Calin, G.A. & Croce, C.M. (2006). *Nat Rev Cancer*, **6,** 857-66.

Calin, G.A., Sevignani, C., Dumitru, C.D., Hyslop, T., Noch, E., Yendamuri, S., Shimizu, M., Rattan, S., Bullrich, F., Negrini, M. & Croce, C.M. (2004). *Proc Natl Acad Sci U S A*, **101,** 2999-3004.

Chang, T.C., Wentzel, E.A., Kent, O.A., Ramachandran, K., Mullendore, M., Lee, K.H., Feldmann, G., Yamakuchi, M., Ferlito, M., Lowenstein, C.J., Arking, D.E., Beer, M.A., Maitra, A. & Mendell, J.T. (2007). *Mol Cell*, **26,** 745-52.

Chang-Zheng, C. (2005). New Eng J Med, **353**, 1768-1771

Corney, D.C., Flesken-Nikitin, A., Godwin, A.K., Wang, W. & Nikitin, A.Y. (2007). *Cancer Res*, **67,** 8433-8.

Crawford, J.R., MacDonald, T.J. & Packer, R.J. (2007). *Lancet Neurol*, **6,** 1073-85.

de Bont, J.M., Packer, R.J., Michiels, E.M., den Boer, M.L. & Pieters, R. (2008). *Neuro Oncol*, **10,** 1040-60.

de Haas, T., Oussoren, E., Grajkowska, W., Perek-Polnik, M., Popovic, M., Zadravec-Zaletel, L., Perera, M., Corte, G., Wirths, O., van Sluis, P., Pietsch, T., Troost, D., Baas, F., Versteeg, R. & Kool, M. (2006). *J Neuropathol Exp Neurol*, **65,** 176-86.

Didiano, D. & Hobert, O. (2008). *Rna*, **14,** 1297-317.

Diederichs, S. & Haber, D.A. (2007). *Cell*, **131,** 1097-108.

Dutta, K.K., Zhong, Y., Liu, Y.T., Yamada, T., Akatsuka, S., Hu, Q., Yoshihara, M., Ohara, H., Takehashi, M., Shinohara, T., Masutani, H., Onuki, J. & Toyokuni, S. (2007). *Cancer Sci*, **98,** 1845-52.

Eberhart, C.G., Kratz, J., Wang, Y., Summers, K., Stearns, D., Cohen, K., Dang, C.V. & Burger, P.C. (2004). *J Neuropathol Exp Neurol*, **63,** 441-9.

Eulalio, A., Huntzinger, E., Nishihara, T., Rehwinkel, J., Fauser, M. & Izaurralde, E. (2009). *Rna*, **15,** 21-32.

Fan, X., Matsui, W., Khaki, L., Stearns, D., Chun, J., Li, Y.M. & Eberhart, C.G. (2006). *Cancer Res*, **66,** 7445-52.

Fan, X., Mikolaenko, I., Elhassan, I., Ni, X., Wang, Y., Ball, D., Brat, D.J., Perry, A. & Eberhart, C.G. (2004). *Cancer Res*, **64,** 7787-93.

Ferretti, E., De Smaele, E., Di Marcotullio, L., Screpanti, I. & Gulino, A. (2005). *Trends Mol Med*, **11,** 537-45.

Ferretti, E., De Smaele, E., Miele, E., Laneve, P., Po, A., Pelloni, M., Paganelli, A., Di Marcotullio, L., Caffarelli, E., Screpanti, I., Bozzoni, I. & Gulino, A. (2008). *Embo J*, **27,** 2616-27.

Ferretti, E., De Smaele, E., Po, A., Di Marcotullio, L., Tosi, E., Espinola, M.S., Di Rocco, C., Riccardi, R., Giangaspero, F., Farcomeni, A., Nofroni, I., Laneve, P., Gioia, U., Caffarelli, E., Bozzoni, I., Screpanti, I. & Gulino, A. (2009). *Int J Cancer*, **124,** 568-77.

Filipowicz, W., Bhattacharyya, S.N. & Sonenberg, N. (2008). *Nat Rev Genet*, **9,** 102-14.

Fuccillo, M., Joyner, A.L. & Fishell, G. (2006). *Nat Rev Neurosci*, **7,** 772-83.

Gajjar, A., Hernan, R., Kocak, M., Fuller, C., Lee, Y., McKinnon, P.J., Wallace, D., Lau, C., Chintagumpala, M., Ashley, D.M., Kellie, S.J., Kun, L. & Gilbertson, R.J. (2004). *J Clin Oncol*, **22,** 984-93.

Gartel, A.L., Feliciano, C. & Tyner, A.L. (2003). *Oncol Res*, **13,** 405-8.

Garzia, L., Andolfo, I., Cusanelli, E., Marino, N., Petrosino, G., De Martino, D., Esposito, V., Galeone, A., Navas, L., Esposito, S., Gargiulo, S., Fattet, S., Donofrio, V., Cinalli, G., Brunetti, A., Vecchio, L.D., Northcott, P.A., Delattre, O., Taylor, M.D., Iolascon, A. & Zollo, M. (2009). *PLoS ONE*, **4,** e4998.

Gilbertson, R.J. & Ellison, D.W. (2008). *Annu Rev Pathol*, **3,** 341-65.

Goodrich, L.V., Milenkovic, L., Higgins, K.M. & Scott, M.P. (1997). *Science*, **277,** 1109-13.

Grimson, A., Farh, K.K., Johnston, W.K., Garrett-Engele, P., Lim, L.P. & Bartel, D.P. (2007). *Mol Cell*, **27,** 91-105.

Hallahan, A.R., Pritchard, J.I., Hansen, S., Benson, M., Stoeck, J., Hatton, B.A., Russell, T.L., Ellenbogen, R.G., Bernstein, I.D., Beachy, P.A. & Olson, J.M. (2004). *Cancer Res*, **64,** 7794-800.

Han, J., Lee, Y., Yeom, K.H., Nam, J.W., Heo, I., Rhee, J.K., Sohn, S.Y., Cho, Y., Zhang, B.T. & Kim, V.N. (2006). *Cell*, **125,** 887-901.

He, L., He, X., Lim, L.P., de Stanchina, E., Xuan, Z., Liang, Y., Xue, W., Zender, L., Magnus, J., Ridzon, D., Jackson, A.L., Linsley, P.S., Chen, C., Lowe, S.W., Cleary, M.A. & Hannon, G.J. (2007). *Nature*, **447,** 1130-4.

Humphreys, D.T., Westman, B.J., Martin, D.I. & Preiss, T. (2005). *Proc Natl Acad Sci U S A*, **102,** 16961-6.

Khvorova, A., Reynolds, A. & Jayasena, S.D. (2003). *Cell*, **115,** 209-16.

Kim, G.J., Park, S.Y., Kim, H., Chun, Y.H. & Park, S.H. (2001). *Cancer Genet Cytogenet*, **129,** 10-6.

Kimura, H., Stephen, D., Joyner, A. & Curran, T. (2005). *Oncogene*, **24,** 4026-36.

Kiriakidou, M., Tan, G.S., Lamprinaki, S., De Planell-Saguer, M., Nelson, P.T. & Mourelatos, Z. (2007). *Cell*, **129,** 1141-51.

Kozaki, K., Imoto, I., Mogi, S., Omura, K. & Inazawa, J. (2008). *Cancer Res*, **68,** 2094-105.

Ladi, E., Nichols, J.T., Ge, W., Miyamoto, A., Yao, C., Yang, L.T., Boulter, J., Sun, Y.E., Kintner, C. & Weinmaster, G. (2005). *J Cell Biol*, **170,** 983-92.

Laws, A.M. & Osborne, B.A. (2004). *Eur J Immunol*, **34,** 726-34.

Lee, A., Kessler, J.D., Read, T.A., Kaiser, C., Corbeil, D., Huttner, W.B., Johnson, J.E. & Wechsler-Reya, R.J. (2005). *Nat Neurosci*, **8,** 723-9.

Lee, Y., Ahn, C., Han, J., Choi, H., Kim, J., Yim, J., Lee, J., Provost, P., Radmark, O., Kim, S. & Kim, V.N. (2003). *Nature*, **425,** 415-9.

Lee, Y., Kim, M., Han, J., Yeom, K.H., Lee, S., Baek, S.H. & Kim, V.N. (2004). *Embo J*, **23,** 4051-60.

Lewis, B.P., Burge, C.B. & Bartel, D.P. (2005). *Cell*, **120,** 15-20.

Li X-N, Patrikh S, Shu Q, Jung H-L, Chow C-W, Perlaky L *et al* (2004). *Clin.Cancer Res* **10**: 1150-1159.

Lodygin, D., Tarasov, V., Epanchintsev, A., Berking, C., Knyazeva, T., Korner, H., Knyazev, P., Diebold, J. & Hermeking, H. (2008). *Cell Cycle*, **7,** 2591-600.

Louvi, A. & Artavanis-Tsakonas, S. (2006). *Nat Rev Neurosci*, **7,** 93-102.

Lund, E., Guttinger, S., Calado, A., Dahlberg, J.E. & Kutay, U. (2004). *Science*, **303,** 95-8.

Lytle, J.R., Yario, T.A. & Steitz, J.A. (2007). *Proc Natl Acad Sci U S A*, **104,** 9667-72.

Marino, S. (2005). *Trends Mol Med*, **11,** 17-22.

Mathonnet, G., Fabian, M.R., Svitkin, Y.V., Parsyan, A., Huck, L., Murata, T., Biffo, S., Merrick, W.C., Darzynkiewicz, E., Pillai, R.S., Filipowicz, W., Duchaine, T.F. & Sonenberg, N. (2007). *Science*, **317,** 1764-7.

Miska, E.A. (2005). *Curr Opin Genet Dev*, **15,** 563-8.

Morlando, M., Ballarino, M., Gromak, N., Pagano, F., Bozzoni, I. & Proudfoot, N.J. (2008). *Nat Struct Mol Biol*, **15,** 902-9.

Perez-Martinez, A., Lassaletta, A., Gonzalez-Vicent, M., Sevilla, J., Diaz, M.A. & Madero, L. (2005). *J Neurooncol*, **71,** 33-8.

Pillai, R.S., Bhattacharyya, S.N. & Filipowicz, W. (2007). *Trends Cell Biol*, **17,** 118-26.

Radtke, F. & Raj, K. (2003). *Nat Rev Cancer*, **3,** 756-67.

Raver-Shapira, N., Marciano, E., Meiri, E., Spector, Y., Rosenfeld, N., Moskovits, N., Bentwich, Z. & Oren, M. (2007). *Mol Cell*, **26,** 731-43.

Rodriguez, A., Griffiths-Jones, S., Ashurst, J.L. & Bradley, A. (2004). *Genome Res*, **14,** 1902-10.

Romer, J.T., Kimura, H., Magdaleno, S., Sasai, K., Fuller, C., Baines, H., Connelly, M., Stewart, C.F., Gould, S., Rubin, L.L. & Curran, T. (2004). *Cancer Cell*, **6,** 229-40.

Rutkowski, S., Bode, U., Deinlein, F., Ottensmeier, H., Warmuth-Metz, M., Soerensen, N., Graf, N., Emser, A., Pietsch, T., Wolff, J.E., Kortmann, R.D. & Kuehl, J. (2005). *N Engl J Med*, **352,** 978-86.

Sakamoto, K., Ohara, O., Takagi, M., Takeda, S. & Katsube, K. (2002). *Dev Biol*, **241,** 313-26.

Schleiermacher, G., Janoueix-Lerosey, I., Combaret, V., Derre, J., Couturier, J., Aurias, A. & Delattre, O. (2003). *Cancer Genet Cytogenet*, **141,** 32-42.

Shimizu, K., Chiba, S., Hosoya, N., Kumano, K., Saito, T., Kurokawa, M., Kanda, Y., Hamada, Y. & Hirai, H. (2000a). *Mol Cell Biol*, **20,** 6913-22.

Shimizu, K., Chiba, S., Saito, T., Kumano, K. & Hirai, H. (2000b). *Biochem Biophys Res Commun*, **276,** 385-9.

Shimojo, H., Ohtsuka, T. & Kageyama, R. (2008). *Neuron*, **58,** 52-64.

Shen Y-M, Meltzer H, Saljooque F, Sang UH (2001). *Dev. Neurosci* **23:** 84-90.

Solecki, D.J., Liu, X.L., Tomoda, T., Fang, Y. & Hatten, M.E. (2001). *Neuron*, **31,** 557-68.

Standart, N. & Jackson, R.J. (2007). *Genes Dev*, **21,** 1975-82.

Stearns, D., Chaudhry, A., Abel, T.W., Burger, P.C., Dang, C.V. & Eberhart, C.G. (2006). *Cancer Res*, **66,** 673-81.

Sun, F., Fu, H., Liu, Q., Tie, Y., Zhu, J., Xing, R., Sun, Z. & Zheng, X. (2008). *FEBS Lett*, **582,** 1564-8.

Takamizawa, J., Konishi, H., Yanagisawa, K., Tomida, S., Osada, H., Endoh, H., Harano, T., Yatabe, Y., Nagino, M., Nimura, Y., Mitsudomi, T. & Takahashi, T. (2004). *Cancer Res*, **64,** 3753-6.

Tarasov, V., Jung, P., Verdoodt, B., Lodygin, D., Epanchintsev, A., Menssen, A., Meister, G. & Hermeking, H. (2007). *Cell Cycle*, **6,** 1586-93.

Tay, Y., Zhang, J., Thomson, A.M., Lim, B. & Rigoutsos, I. (2008). *Nature*, **455,** 1124-8.

Tazawa, H., Tsuchiya, N., Izumiya, M. & Nakagama, H. (2007). *Proc Natl Acad Sci U S A*, **104,** 15472-7.

Thiele, CJ, (1998). Neuroblastoma: In (Ed.) Masters, J. Human Cell Culture. Lancaster, UK: Kluwer Academic Publishers. Vol **1**, p 21-53.

Vasudevan, S. & Steitz, J.A. (2007). *Cell*, **128,** 1105-18.

Vasudevan, S., Tong, Y. & Steitz, J.A. (2007). *Science*, **318,** 1931-4.

Ventura, A., Young, A.G., Winslow, M.M., Lintault, L., Meissner, A., Erkeland, S.J., Newman, J., Bronson, R.T., Crowley, D., Stone, J.R., Jaenisch, R., Sharp, P.A. & Jacks, T. (2008). *Cell*, **132,** 875-86.

Wakiyama, M., Takimoto, K., Ohara, O. & Yokoyama, S. (2007). *Genes Dev*, **21,** 1857-62.

Wang, Q., Li, H., Liu, N., Chen, X.Y., Wu, M.L., Zhang, K.L., Kong, Q.Y. & Liu, J. (2008). *Neurosci Lett*, **438,** 168-73.

Wang, V.Y. & Zoghbi, H.Y. (2001). *Nat Rev Neurosci*, **2,** 484-91.

Wang, X. (2006). *Nucleic Acids Res*, **34,** 1646-52.

Wei, J.S., Song, Y.K., Durinck, S., Chen, Q.R., Cheuk, A.T., Tsang, P., Zhang, Q., Thiele, C.J., Slack, A., Shohet, J. & Khan, J. (2008). *Oncogene*, **27,** 5204-13.

Welch, C., Chen, Y. & Stallings, R.L. (2007). *Oncogene*, **26,** 5017-22.

Wetmore, C., Eberhart, D.E. & Curran, T. (2001). *Cancer Res*, **61,** 513-6.

Wu, L. & Belasco, J.G. (2008). *Mol Cell*, **29,** 1-7.

Wu, L., Fan, J. & Belasco, J.G. (2006). *Proc Natl Acad Sci U S A*, **103,** 4034-9.

Yamakuchi, M., Ferlito, M. & Lowenstein, C.J. (2008). *Proc Natl Acad Sci U S A*, **105,** 13421-6.

Yang, Z.J., Ellis, T., Markant, S.L., Read, T.A., Kessler, J.D., Bourboulas, M., Schuller, U., Machold, R., Fishell, G., Rowitch, D.H., Wainwright, B.J. & Wechsler-Reya, R.J. (2008). *Cancer Cell*, **14,** 135-45.

Zhang, B., Pan, X., Cobb, G.P. & Anderson, T.A. (2007). *Dev Biol*, **302,** 1-12.